# Analysis of hepatitis C virus-specific CD8+ T-cells with HLA-A*24 tetramers during phlebotomy and interferon therapy for chronic hepatitis C

KYOSUKE KAJI, YASUNARI NAKAMOTO and SHUICHI KANEKO

Department of Gastroenterology, Graduate School of Medicine, Kanazawa University, Kanazawa, Japan

Received May 1, 2007; Accepted June 25, 2007

**Abstract.** Hepatitis C virus (HCV)-specific, HLA class I-restricted, CD8-positive (CD8+) T lymphocytes are thought to contribute to viral clearance as well as liver disease in chronic hepatitis C. For the patients who do not respond to interferon (IFN) therapy, phlebotomy can be used as a tool to reduce inflammation and lower transaminase levels; however, the immunological aspects have not been clearly defined. In this study, we evaluated the HCV-specific CD8+ T-cell responses during phlebotomy and IFN therapy using HLA-A*24 tetramers in 6 Japanese patients with chronic hepatitis C. During phlebotomy, 4 of the 6 cases achieved a biochemical response, but there was no clear correlation between its efficacy and HCV viral loads or changes in frequencies or activation status of tetramer-positive T-cells. In contrast, the frequencies of tetramer-positive cells and the proportions of T-cells expressing activation marker HLA-DR were higher in sustained viral responders than in transient responders to IFN therapy. Furthermore, expression of the activation marker was enhanced in the initial period of IFN therapy. The results suggest that the immunological aspects of phlebotomy obviously differ from those of IFN therapy and these differences may provide clues as to a therapeutic strategy of their combination for patients who do not respond to IFN monotherapy.

## Introduction

Interferon (IFN) treatment is a radical therapy for the elimination of hepatitis C virus (HCV), but many patients do not respond to it; so called 'non-responders'. There have been recent advances in treatment, such as combination therapy with Peginterferon α-2a or α-2b and ribavirin (1-4). To date, there are no therapies for HCV elimination with a sufficiently high success rate and low rate of adverse events.

For non-responders to IFN therapy, secondary treatment is needed to lower serum transaminase levels, slow the progression of fibrosis and reduce the occurrence of hepatocellular carcinoma (5). Phlebotomy is one of the treatments used to reduce inflammation and lower serum transaminase levels (6).

Several studies have examined the correlation between HCV and iron levels. Smith *et al* reported that the progression of fibrosis is faster in patients with chronic hepatitis C with congenital hemochromatosis than in those with normal iron levels (7). Fontana *et al* reported that combination therapy with IFN and phlebotomy may be more effective than IFN monotherapy in patients with chronic hepatitis C (8). We reported the hemosiderin deposition may be a predictive parameter for the efficacy of IFN therapy (9). Mandishona *et al* reported that excess iron may promote the occurrence of hepatocellular carcinoma (10).

The mechanism by which phlebotomy decreases transaminase levels is thought to involve a decrease in the toxic effects of superoxide produced by iron excess (11). However, no studies have been reported regarding the immunological effects of phlebotomy that may be important in mitigating liver injury.

HCV-specific CD8+ cytotoxic T lymphocytes (CTLs) contribute to viral clearance in acute, self-limited hepatitis C as well as to liver cell injury in the more frequent cases with chronic hepatitis C (12-16). In a study using HLA-A*24 tetramer, we previously showed that a close correlation exists between the HCV-specific CD8+ T-cell profile and hepatic fibrosis in HCV-infected Japanese patients, most of whom are HLA-A*24 positive (17). In this study, we analyzed HCV-specific CD8+ T-cell responses during phlebotomy and IFN therapy and observed a correlation between changes in the HCV-specific CD8+ T-cell profile and the therapeutic effects of each treatment.

## Materials and methods

*Patients.* Patients with chronic hepatitis C presented at Kanazawa University Hospital between June 2000 and June 2001 were included in this study. Their selection and diagnosis were based on the following criteria: 1) age from 20 to 70

*Correspondence to*: Dr Shuichi Kaneko, Department of Gastroenterology, Graduate School of Medicine, Kanazawa University, 13-1 Takara-Machi, Kanazawa 920-8641, Japan
E-mail: skaneko@m-kanazawa.jp

*Key words:* chronic hepatitis C, phlebotomy, interferon therapy, tetramers, HLA-A*24

Table I. Clinical characteristics of patients.

| Patients | Age (years) | Sex (M/F) | HCV Serogroup | HCV-RNA (KIU/ml) | ALT (IU/l) | HAI Stage (F) | HAI Grade (A) | ALT change during phlebotomy | Response to IFN therapy |
|---|---|---|---|---|---|---|---|---|---|
| 1 | 47 | F | 2 | 69 | 40 | 1 | 1 | Not decreased | SVR |
| 2 | 60 | M | 2 | 88 | 104 | 3 | 2 | Decreased | TVR |
| 3 | 43 | M | 1 | >500 | 97 | 3 | 2 | Decreased | TVR |
| 4 | 65 | M | 1 | 1.9 | 80 | 1 | 1 | Decreased | SVR |
| 5 | 55 | M | 2 | 0.7 | 39 | 3 | 2 | Decreased | SVR |
| 6 | 51 | M | 2 | >500 | 110 | 1 | 1 | Not decreased | TVR |

Serum HCV RNA was quantified with the Amplicore HCV Monitor ver.3. HAI, histological activity index; SVR, sustained viral responder; TVR, transient viral responder.

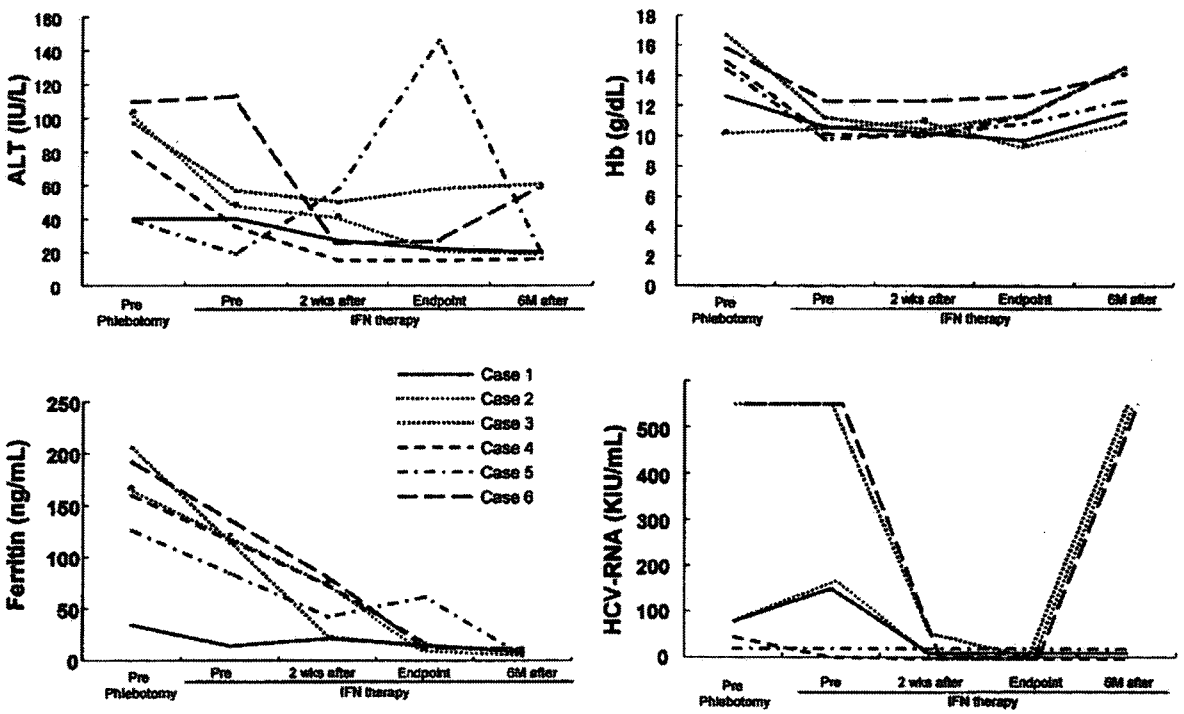


Figure 1. Trends over time for alanine aminotransferase (ALT), hemoglobin, ferritin and HCV-RNA levels during phlebotomy and interferon (IFN) therapy in patients with chronic hepatitis C. Phlebotomy was performed by removing 200 to 400 ml blood per session, once or twice weekly. The sessions were continued until achieving the target levels of hemoglobin (10 g/dl) and/or ferritin (10 ng/ml). After achieving the target levels, IFN-α-2b was administered at a dose of 6 to 10 MU per day for 2 weeks and then 3 times a week for 22 weeks. Each line indicates a single patient.

years; 2) elevated serum aminotransferase (ALT; >50 IU/l) at least once within 1 year; 3) hemoglobin greater than 13.0 g/dl in males or greater than 11.0 g/dl in females; 4) no liver cirrhosis; and 5) HLA-A*24 positive. All cases provided written informed consent.

*Phlebotomy and IFN therapy.* Phlebotomy was performed by removing 200 to 400 ml blood per session, once or twice weekly. The sessions were continued until achieving the target level of hemoglobin (10 g/dl) and/or ferritin (10 ng/ml). After achieving the target level, IFN-α-2b was administered at a dose of 6 to 10 MU per day for 2 weeks and then 3 times a week for 22 weeks.

Complete blood cell count, liver function tests, HCV-RNA determinations and T-cell analysis were performed pre-phlebotomy, just before IFN administration, 2 weeks after IFN therapy, immediately after IFN therapy and 6 months after IFN administration.

Patients whose transaminases decreased during phlebotomy, were recorded as biochemical responders and the others as non-responders. With respect to the HCV-RNA level, patients whose HCV-RNA levels were undetectable both at the end-points of IFN therapy and even at 6 months after the IFN therapy completion were designated as sustained viral responders (SVR) and those whose HCV-RNA were undetectable at the end point of IFN therapy but reappeared 6 months after the end of IFN therapy were designated as transient viral responders (TVR) (1).

*Synthesis of HLA-A*2402-peptide tetramers.* Five peptides were selected to synthesize HLA-A*2402-peptide tetramers (17): HCV E2 717-725 (EYVLLLFLL), NS3 1292-1300

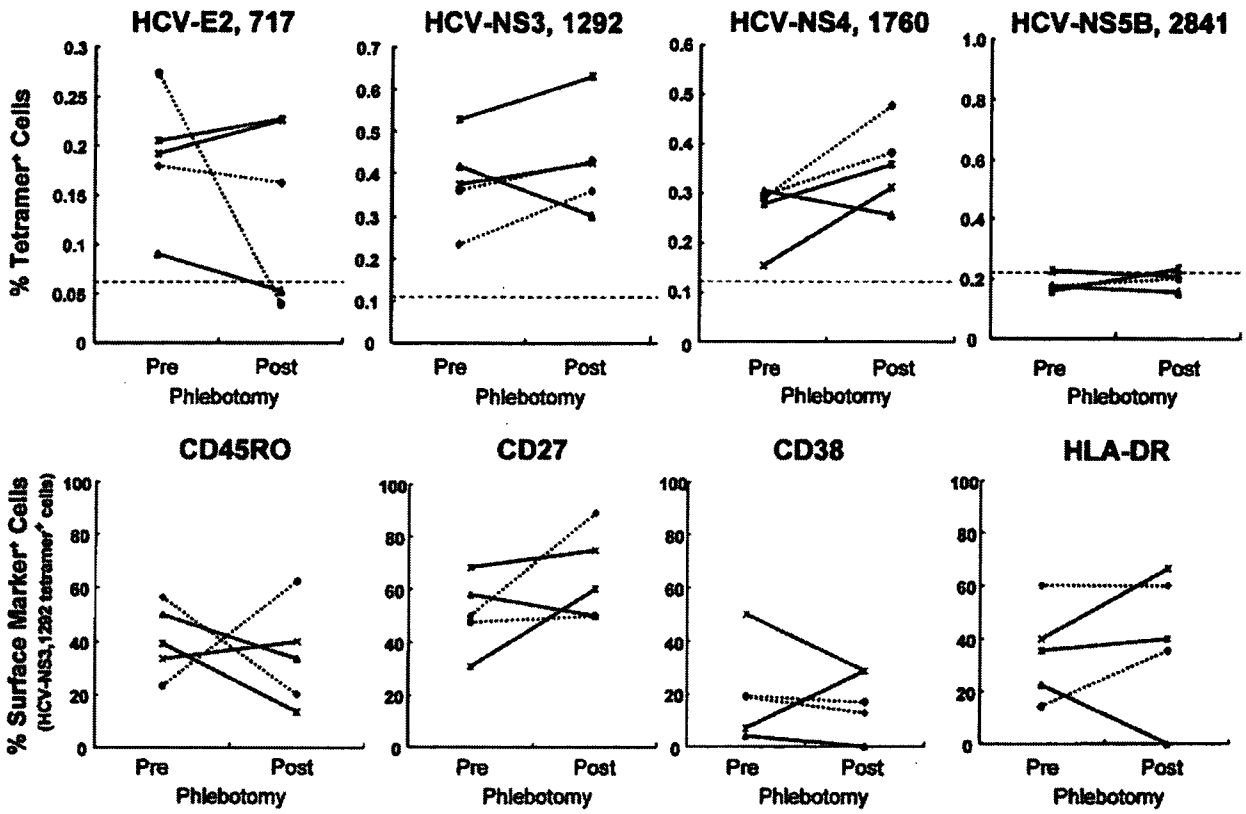


Figure 2. Changes in frequencies of four types of HLA-A*24 tetramer-positive cells and surface markers of tetramer HCV-NS3, 1292-positive cells during phlebotomy. Solid lines represent biochemical responders to phlebotomy and broken lines represent biochemical non-responders (subjects whose ALT did not decrease during phlebotomy). Horizontal broken lines indicate the cut-off value for each HLA tetramer, as mentioned in Materials and methods. There was no correlation between the biochemical effects of phlebotomy and the frequencies of tetramer-positive T-cells or the phenotypes of tetramer-positive cells.

(TYSTYGKFL), NS4 1760-1768 (FWAKHMWNF), NS5B 2841-2849 (RMILMTHFF) and NS5B 2870-2878 (CYSIEPLDL). Three of them, E2 717-725, NS3 1292-1300 and NS5B 2870-2878 were selected because they have been reported to bind to HLA-A*24 with good affinity ($IC_{50}$ <500 nM) in a direct peptide binding assay (18). The other two peptides were chosen because they were conserved within the reported major HCV genotypes 1a and 1b sequences (19-21).

The cut-off values for positive staining with the tetramers was 2 SD above the mean for all control subjects studied previously (17): 0.064% for tetramer HCV-E2.717, 0.11% for tetramer HCV-NS3.1292, 0.12% for tetramer HCV-NS4 1760, 0.22% for tetramer HCV-NS5B.2841 and 0.10% for tetramer HCV-NS5B.2870.

*Tetramer staining and flow cytometry*. Peripheral blood mononuclear cells (PBMCs) were isolated from heparinized venous blood by separation using Ficoll-Hypaque (Sigma Chemical Co., St. Louis, MO) density gradient centrifugation. Freshly isolated PBMCs were stained with tetrameric complexes and antibodies and were then analyzed. The following monoclonal antibodies (mAbs) were used; anti-CD8-Cy-Chrome (CyC) (HIT8a), anti-CD-4-Allophycocyanin (APC) (SK3), anti-CD14-APC (MΦP9), anti-CD19-APC (SJ25C1), anti-CD45RA-FITC (HI100), anti-CD27-FITC (M-T271), anti-CD38-RITC (HIT2) and anti-HLA-DR-FITC (L243) (BD PharMingen, Sand Diego, CA). Freshly isolated cells ($1x10^6$) were washed, resuspended in 200 $\mu$l PBS without calcium and phosphate, and stained with 40 $\mu$g/ml of tetrameric complexes for 30 min at room temperature. Subsequently, antibodies against cell surface proteins were added and incubated for an additional 30 min at room temperature. Cells were washed, fixed with 1% formalin/PBS, and analyzed on a FACSCalibur™ flow cytometer. Data were analyzed with CELLQuest™ software (Becton Dickinson, San Jose, CA).

## Results

*Clinical course*. The 6 cases studied included 5 males and 1 female (Table I). They ranged in age from 43 to 60 years. Of the patients, 4 had serogroup 2 HCV and 2 had serogroup 1 HCV. Serogroup 1 HCV is known to be more common than serogroup 2 in Japan (22).

Phlebotomies were performed in all cases without significant adverse events over a period of 7 to 20 days. Eventually, the total volume of blood removed was from 600 to 2800 ml (mean = 1600 ml). In 4 of the 6 cases, transaminase levels decreased during phlebotomy, but there was no effect of phlebotomy on HCV viral loads (Fig. 1).

IFN treatments were associated with lower HCV viral loads. At the endpoints of the treatments, HCV-RNA disappeared from sera of all 6 cases. Six months after IFN therapy, HCV reappeared in 3 cases (transient viral responder,

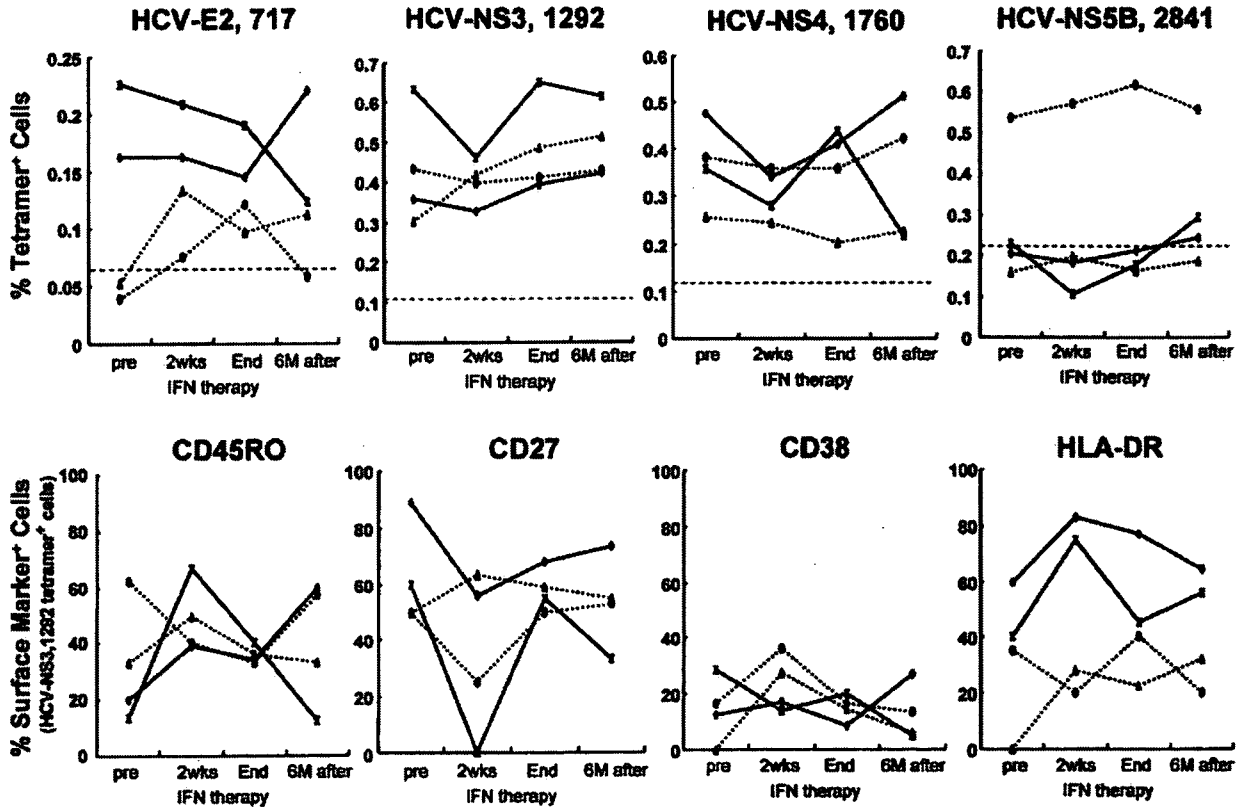


Figure 3. Changes in frequencies of four types of HLA-A*24 tetramer-positive cells and surface markers of tetramer HCV-NS3, 1292-positive cells during IFN therapy. Solid lines represent viral responders to IFN therapy (sustained viral responders, SVRs) and the broken lines represent transient viral responders (TVRs) whose HCV reappeared within 6 months after the end of IFN therapy. Horizontal broken lines in the upper four panels indicate the cut-off values for HLA tetramers, as mentioned in Materials and methods. The HLA-DR positive rates among tetramer (HCV-NS3, 1292)-positive cells were higher in SVRs than in TVRs at the start of IFN treatment and further increased after 2 weeks of IFN therapy.

TVR) and in the other 3 cases HCV remained below the detection limit (sustained viral responder, SVR) (Fig. 1).

*HCV-specific CD8⁺ T-cell responses during phlebotomy.* During phlebotomy, we analyzed HCV-specific CD8⁺ T-cell responses in 5 cases (patients 1, 3, 4, 5, and 6); and among them, 3 cases were biochemical responders to phlebotomy and the other 2 cases were non-responders (Table I and Fig. 2). The numbers of HLA-A*24 tetramer-positive T-cells were above the cut-off levels for all 3 of the tetramers, HCV-E2.717, HCV-NS3.1292, and HCV-NS4.1760. There was no correlation between the biochemical effects of phlebotomy and the frequencies of tetramer-positive T-cells. We also analyzed the phenotypes of tetramer-positive cells by staining CD45RO, CD27, CD38 and HLA-DR, but we did not observe a correlation between the biochemical effects and the phenotypes. The data indicate that phlebotomy displayed its therapeutic effects for the patients with chronic hepatitis C without affecting the frequencies and phenotypes of HCV-specific CD8⁺ T-cell responses.

*HCV-specific CD8⁺ T-cell responses during IFN therapy.* During and after IFN therapy, we analyzed HCV-specific CD8⁺ T-cell responses in 2 sustained responders (patients 1 and 5) and 2 transient responders (patients 3 and 6) (Table I and Fig. 3). The three different tetramer-positive T-cells, HCV-E2.717, HCV-NS3. 1292 and HCV-NS4.1760 were also detectable at levels above the cut-off during IFN therapy. The frequencies of HCV-E2.717 positive cells were higher in SVR patients than in TVR patients before, during and 6 months after IFN therapy. Interestingly, activation marker HLA-DR positive rates among tetramer-positive cells were higher in SVR patients than in TVR patients before IFN treatment and increased further after 2 weeks of IFN therapy and beyond. These results demonstrate that IFN therapy exerted its beneficial effects on the patients with high frequencies of the HCV-specific CD8⁺ T-cells and enhanced expression of the activation markers, suggesting that the efficacy of IFN therapy for chronic hepatitis C may be mediated by the virus-specific T-cell dependent immunity.

## Discussion

For patients with chronic hepatitis C who do not respond to IFN therapy, other treatments to reduce inflammation and decrease transaminase levels are indicated to slow the progression of fibrosis and to lower the incidence of hepatocellular carcinoma. Phlebotomy is one of the therapies used to decrease the inflammation in the liver. In this study, we analyzed HCV-specific CD8⁺ T-cell responses in 6 patients with chronic hepatitis C treated by phlebotomy followed by IFN therapy. HLA-A*24 tetramer HCV-E2.717ÅAHCV-

NS3.1292 and HCV-NS4.1760 positive T-cells were detected at levels above the cut-off values. During phlebotomy, there was no correlation between the effectiveness of treatments and virological and immunological parameters, such as HCV viral loads, frequencies of tetramer-positive cells and their phenotypes of activation status, although 4 of the 6 cases achieved biochemical improvement. During IFN therapy, interestingly, the frequencies of HCV-E2.717 positive cells were higher in SVR patients than in TVR patients. Additionally, proportions of HLA-DR positive cells among tetramer-positive cells were higher in SVRs than in TVRs at the start of treatment; the proportions increased after 2 weeks of IFN administration and remained elevated during the follow-up periods.

Phlebotomy is thought to be effective by correcting iron excess in chronic hepatitis C. The previous studies have reported that the progression of fibrosis is faster in chronic hepatitis C patients with congenital hemochromatosis (7), that combination therapy with IFN and phlebotomy may be more effective than IFN monotherapy (8), that hemosiderin deposition may be a predictive factor for IFN efficacy (9) and that dietary iron overload may be a risk factor for hepatocellular carcinoma (10). Inhibition of the toxic effects of superoxide or excess iron has been postulated as a mechanism underlying the therapeutic effects of phlebotomy (11); however, the possible involvement of immunological mechanisms had not been addressed.

Recently developed HLA-class I peptide tetramers, consisting of fluorescently-tagged tetrameric complexes of HLA heavy chains folded around epitope peptides, allow the sensitive and precise enumeration of T lymphocytes with specific T-cell antigen receptors (TCR) (23,24). With regard to HCV infection, this technology revealed that epitope-specific $CD8^+$ T lymphocytes are not only detectable in *in vitro* expanded $CD8^+$ T lymphocytes but also in freshly isolated PBMCs at more than 10-fold higher frequencies than those previously reported (25). Furthermore, the technology has facilitated the phenotypic, functional and molecular analysis of virus-specific immune responses at the single cell level (25). Additionally, by means of tetramers, the relative frequencies of T lymphocytes specific for different epitopes were observed to change during the course of viral infection (26). We have reported the frequency, phenotype and clinical significance of HCV-specific $CD8^+$ T lymphocytes using five different HLA-A*24 tetramers in HCV-infected Japanese patients (17).

Manfras *et al* reported that increased oligoclonality of circulating $CD8^+$ T-cells in chronic HCV infection was an indicator of a poor clinical reponse to IFN-α therapy; that IFN-α therapy enhanced the differentiation of $CD8^+$ T-cells towards a late differentiation phenotype ($CD28^-$ $CD57^+$); and that in cases of virus elimination, there was disappearance of expanded, terminally-differentiated $CD8^+$ cells (27). In our study, we found that the HLA-DR positive $CD8^+$ T-cells increased after 2 weeks of IFN therapy. On the other hand, during phlebotomy, there was no correlation between the improvement of liver function parameters and the frequencies of tetramer-positive cells or changes in the levels of activation markers. These findings may indicate that the mechanisms of phlebotomy and IFN therapy differ immunologically.

This is the first study to observe the alteration of HCV-specific T-cells, not only during IFN therapy, but also during the phlebotomy and the findings suggest that there may be important differences in their immunological aspects. The use of a combination of therapies which have different but complimentary mechanisms may be more beneficial for the treatment of chronic hepatitis C.

## References


1. Fried MW, Shiffman ML, Reddy KR, *et al*: Peginterferon alfa-2a plus ribavirin for chronic hepatitis C virus infection. N Engl J Med 347: 975-982, 2002.
2. Heathcote EJ, Shiffman ML, Cooksley WG, *et al*: Peginterferon alfa-2a in patients with chronic hepatitis C and cirrhosis. N Engl J Med 343: 1673-1680, 2000.
3. Davis GL, Esteban-Mur R, Rustgi V, *et al*: Interferon alfa-2b alone or in combination with ribavirin for the treatment of relapse of chronic hepatitis C. International Hepatitis Interventional Therapy Group. N Engl J Med 339: 1493-1499, 1998.
4. McHutchison JG, Gordon SC, Schiff ER, *et al*: Interferon alfa-2b alone or in combination with ribavirin as initial treatment for chronic hepatitis C. Hepatitis Interventional Therapy Group. N Engl J Med 339: 1485-1492, 1998.
5. Tarao K, Rino Y, Ohkawa S, *et al*: Association between high serum alanine aminotransferase levels and more rapid development and higher rate of incidence of hepatocellular carcinoma in patients with hepatitis C virus-associated cirrhosis. Cancer 86: 589-595, 1999.
6. Hayashi H, Takikawa T, Nishimura N, Yano M, Isomura T and Sakamoto N: Improvement of serum aminotransferase levels after phlebotomy in patients with chronic active hepatitis C and excess hepatic iron. Am J Gastroenterol 89: 986-988, 1994.
7. Smith BC, Gorve J, Guzail MA, Day CP, Daly AK, Burt AD and Bassendine MF: Heterozygosity for hereditary hemochromatosis is associated with more fibrosis in chronic hepatitis C. Hepatology 27: 1695-1699, 1998.
8. Fontana RJ, Israel J, LeClair P, *et al*: Iron reduction before and during interferon therapy of chronic hepatitis C: results of a multicenter, randomized, controlled trial. Hepatology 31: 730-736, 2000.
9. Kaji K, Nakanuma Y, Harada K, Sakai A, Kaneko S and Kobayashi K: Hemosiderin deposition in portal endothelial cells is a histologic marker predicting poor response to interferon-alpha therapy in chronic hepatitis C. Pathol Int 47: 347-352, 1997.
10. Mandishona E, MacPhail AP, Gordeuk VR, Kedda MA, Paterson AC, Rouault TA and Kew MC: Dietary iron overload as a risk factor for hepatocellular carcinoma in Black Africans. Hepatology 27: 1563-1566, 1998.
11. Kato J, Kobune M, Nakamura T, *et al*: Normalization of elevated hepatic 8-hydroxy-2'-deoxyguanosine levels in chronic hepatitis C patients by phlebotomy and low iron diet. Cancer Res 61: 8697-8702, 2001.
12. Cerny A and Chisari FV: Immunological aspects of HCV infection. Intervirology 37: 119-125, 1994.
13. Chang KM, Rehermann B and Chisari FV: Immunopathology of hepatitis C. Springer Semin Immunopathol 19: 57-68, 1997.
14. Gruner NH, Gerlach TJ, Jung MC, *et al*: Association of hepatitis C virus-specific $CD8^+$ T-cells with viral clearance in acute hepatitis C. J Infect Dis 181: 1528-1536, 2000.
15. Rehermann B and Chisari FV: Cell mediated immune response to the hepatitis C virus. Curr Top Microbiol Immunol 242: 299-325, 2000.
16. Lechner F, Gruener NH, Urbani S, *et al*: $CD8^+$ T lymphocyte responses are induced during acute hepatitis C virus infection but are not sustained. Eur J Immunol 30: 2479-2487, 2000.
17. Nakamoto Y, Kaneko S, Takizawa H, Kikumoto Y, Takano M, Himeda Y and Kobayashi K: Analysis of the CD8-positive T-cell response in Japanese patients with chronic hepatitis C using HLA-A*2402 peptide tetramers. J Med Virol 70: 51-61, 2003.
18. Kondo A, Sidney J, Southwood S, *et al*: Prominent roles of secondary anchor residues in peptide binding to HLA-A*24 human class I molecules. J Immunol 155: 4307-4312, 1995.
19. Kato N, Hijikata M, Ootsuyama Y, Nakagawa M, Ohkoshi S, Sugimura T and Shimotohno K: Molecular cloning of the human hepatitis C virus genome from Japanese patients with non-A, non-B hepatitis. Proc Natl Acad Sci USA 87: 9524-9528, 1990.

20. Choo QL, Richman KH, Han JH, *et al*: Genetic organization and diversity of the hepatitis C virus. Proc Natl Acad Sci USA 88: 2451-2455, 1991.
21. Takamizawa A, Mori C, Fuke I, *et al*: Structure and organization of the hepatitis C virus genome isolated from human carriers. J Virol 65: 1105-1113, 1991.
22. Yamada G, Tanaka E, Miura T, *et al*: Epidemiology of genotypes of hepatitis C virus in Japanese patients with type C chronic liver diseases: a multi-institution analysis. J Gastroenterol Hepatol 10: 538-545, 1995.
23. Altman JD, Moss PA, Goulder PJ, *et al*: Phenotypic analysis of antigen-specific T lymphocytes. Science 274: 94-96, 1996.
24. Ogg GS and McMichael AJ: HLA-peptide tetrameric complexes. Curr Opin Immunol 10: 393-396, 1998.
25. Doherty PC and Christensen JP: Accessing complexity: the dynamics of virus-specific T-cell responses. Annu Rev Immunol 18: 561-592, 2000.
26. Blattman JN, Sourdive DJ, Murali-Krishna K, Ahmed R and Altman JD: Evolution of the T-cell repertoire during primary, memory and recall responses to viral infection. J Immunol 165: 6081-6090, 2000.
27. Manfras BJ, Weidenbach H, Beckh KH, *et al*: Oligoclonal CD8$^+$ T-cell expansion in patients with chronic hepatitis C is associated with liver pathology and poor response to interferon-alpha therapy. J Clin Immunol 24: 258-271, 2004.

# Hepatitis B virus X protein overcomes oncogenic RAS-induced senescence in human immortalized cells

Naoki Oishi,[1,2] Khurts Shilagardi,[1] Yasunari Nakamoto,[2] Masao Honda,[2] Shuichi Kaneko[2] and Seishi Murakami[1,3]

[1]Department of Signal Transduction, Cancer Research Institute; [2]Department of Disease Control and Homeostasis, Graduate School of Medicine, Kanazawa University, 13-1 Takara-machi, Kanazawa 920-0934, Japan

(Received February 23, 2007/Revised June 12, 2007/Accepted June 25, 2007/Online publication August 19, 2007)

**Chronic infection with hepatitis B virus (HBV) is a major risk factor for hepatocellular carcinoma. The HBV X protein (HBx) is thought to have oncogenic potential, although the molecular mechanism remains obscure. Pathological roles of HBx in the carcinogenic process have been examined using rodent systems and no report is available on the oncogenic roles of HBx in human cells *in vitro*. We therefore examined the effect of HBx on immortalization and transformation in human primary cells. We found that HBx could overcome active RAS-induced senescence in human immortalized cells and that these cells could form colonies in soft agar and tumors in nude mice. HBx alone, however, could contribute to neither immortalization nor transformation of these cells. In a population doubling analysis, an N-terminal truncated mutant of HBx, HBx-D1 (amino acids 51–154), which harbors the coactivation domain, could overcome active RAS-induced cellular senescence, but these cells failed to exhibit colonigenic and tumorigenic abilities, probably due to the low expression level of the protein. By scanning a HBx expression library of the clustered-alanine substitution mutants, the N-terminal domain was found to be critical for overcoming active RAS-induced senescence by stabilizing full-length HBx. These results strongly suggest that HBx can contribute to cardinogenesis by overcoming active oncogene-induced senescence. (*Cancer Sci* 2007; 98: 1540–1548)**

Chronic infection with HBV is a major risk factor for HCC worldwide. HBV belongs to the Hepadnavirus family. Its genome is a 3.2-kb, circular, partially double-stranded DNA molecule with four overlapping open reading frames: PC-C, PS-S, P and X.[1] The HBV genome, which is converted to covalently closed circular DNA in the nucleus after infection, serves as the template for transcription, generating the four viral transcripts that encode the HBV core and polymerase polypeptides, the large surface antigen polypeptide, the middle and major surface antigen polypeptides, and the HBx polypeptide. HBV replicates by reverse transcription of viral pregenomic 3.5-kb RNA using the HBV polymerase that catalyzes RNA-dependent DNA synthesis and DNA-dependent DNA synthesis.[1,2] It is converted into the 3.2-kb partially double-stranded genomic DNA inside the viral capsid.

The critical role of HBV chronic infection in HCC has been well established etiologically, whereas the mechanism by which HBV causes transformation of hepatocytes remains unclear.[3–5] HBx has long been suspected of playing a positive role in hepatocarcinogenesis, as avian hepadnaviruses missing the X open reading frame seem not to be associated with HCC. HBx consists of 154 aa and is a multifunctional regulator that modulates many host cell functions through its interactions with a variety of host factors.[5] HBx consists of both a negative regulatory domain[6] and a coactivation domain that is required for the augmentation of virus and host genes.[7,8] HBx was reported to transform rodent immortal cells *in vitro*,[9,10] and a high incidence of HCC has been reported in transgenic mice overexpressing HBx.[11,12] However, the functional role of HBx in the transformation is still controversial. Some independent groups proposed collaborating roles of HBx in the hepatocarcinogenic process.[13–15] Although these reports are informative, all were experimentally assessed in rodent systems. Because mouse and human primary cells have different telomere biology,[16] DNA damage check point control mechanisms and cell cycle progression,[17,18] developing a human system to address the functional role of HBx is critically important. Here we report that we established human fibroblast cells stably expressing HBx protein and analyzed the effects of HBx expression on the ability to confer an immortal phenotype and tumorigenic potential.

## Materials and Methods

**Retroviral vectors.** All constructs for the expression of HBx (subtype adr) proteins, pNKF-HBx (aa 1–154), pNKF-HBx-D1 (aa 1–50) and pNKF-HBx-D5 (aa 51–154) have been described previously.[8] The retrovirus vectors pBabe-puro, hygro, puro-H-RAS$^{V12}$ hygro-hTERT and pWZL-blast were kindly provided by W. C. Hahn (Dana-Farber Cancer Institute, Harvard).[19,20] To construct pBabe-blast, the blasticidin S cDNA of pWZL-blast was used as a template to amplify the PCR products of blasticidin S with the primer set of AAGCTTACCATGGCCAAGCCTTTGT and ATCGATTTAGCCCTCCCACACATAA, generating an artificial *Hind*III site at the 5-end and a *Cla*I site at the 3′-end, respectively. The HBx cDNA of pNKF-HBx was used as a template to amplify the PCR products of HBx with a primer set of TGATCAATGGACTACAAAGACGAT and CTCGAGAGAT-CTTTAATTAATTAA, generating an artificial *Fba*I site at the 5-end and an *Xho*I site at the 3′-end, respectively. The PCR products were digested and inserted into the *Bam*HI and *Sal*I sites of the pBabe-blast vector. The *Eco*RI and *Bgl*II fragments of HBx-D1 and HBx-D5 from pNKF-HBx-D1 and pNKF-HBx-D5 were, respectively, inserted into the *Eco*RI and *Bgl*II sites of the pBabe-blast-HBx vectors. An alanine scanning method was applied to construct a series of HBx clustered alanine substitution mutants (designated 'cm') by site-directed mutagenesis. The mutagenesis was carried out using a splicing PCR method with all of the mutated oligonucleotide primer sets. The target sequence of seven aa residues was changed to AAASAAA, and all of the HBx-encoding DNA fragments bearing the clustered mutations were introduced into the *Eco*RI and *Bam*HI sites of pNKFLAG, generating the pNKF-Xcm1 to pNKF-Xcm21 constructs. The

[3]To whom correspondence should be addressed.
E-mail: semuraka@kenroku.kanazawa-u.ac.jp

Abbreviations: aa, amino acid; DMEM, Dulbecco's modified Eagle's medium; HBV, hepatitis B virus; HBx, hepatitis B virus X protein; HCC, hepatocellular carcinoma; hTERT, human telomerase reverse transcriptase; OIS, oncogene-induced senescence; PCR, polymerase chain reaction; PD, population doubling; SA-β-gal, senescence-associated β-galactosidase; SDS-PAGE, sodium dodecylsulfate–polyacrylamide gel electrophoresis.



doi: 10.1111/j.1349-7006.2007.00579.x

*Eco*RI and *Bgl*II fragments of HBx-cm1 to HBx-cm21 from pNKF-Xcm1 to pNKF-Xcm21 were, respectively, inserted into the *Eco*RI and *Bgl*II sites of the pBabe-blast-HBx vectors. All of the constructs were sequenced by the dideoxy method using the *Taq* sequencing primer kit and a DNA sequencer (370A; Applied Biosystems).

**Virus production and cell lines.** Amphotropic retroviruses were produced by transfection of the 293T producer cell line with a retroviral vector and a vector encoding replication-defective helper viruses, pCL-Ampho (Imgenex), using FuGENE 6 transfection reagent (Roche Applied Science) according to the manufacturer's recommendations. Two days after the transfection, culture supernatants were collected, filtered, supplemented with 4 μg/mL polybrene, and used for infection. Two days after the infection, drug selection of infected cells was started, and the selected populations were used in all of the experiments. Infected cell populations were selected in puromycin (1.0 μg/mL), blasticidin S (4 μg/mL) and hygromycin (80 μg/mL) for up to 2 weeks.

**Cell culture.** Human lung fibroblasts (TIG3) from the Japanese Collection of Research Bioresources were maintained in DMEM with 10% heat-inactivated fetal bovine serum (JRH Biosciences). Human foreskin fibroblasts, BJ and BJ-hTERT-LT-ST-H-RAS$^{V12}$ cells were maintained as described previously.[19] These human fibroblasts were not clonal and were maintained as populations. BJ cells and TIG3 cells have a finite lifespan, and were used at PD between 25 and 35. PD were determined using the formula:

$$PD = Log(Nf/Ni)/Log2,$$

where Nf = the number of cells counted and Ni = the number of cells seeded. Comparisons of means and standard deviations were carried out using the unpaired *t*-test.

**Western blot analysis.** Cells were harvested, washed with phosphate-buffered saline (–), and sonicated in a lysis buffer (50 mM Tris-HCl [pH 7.4], 200 mM NaCl, 1 mM ethylenediaminetetraacetic acid, 10% glycerol, 1 mM phenylmethylsulfonyl fluoride, 10 μg/mL leupeptin, 10 μg/mL aprotinin and 10 μg/mL dithiothreitol). Total lysates were fractionated by SDS-PAGE, transferred onto nitrocellulose membranes and subjected to western blot analysis with antibodies. Anti-FLAG M2 antibody and anti-β-actin antibody were from Sigma. Anti-RAS antibody F-235 (sc-29), anti-p53 antibody DO-1 (sc-126) and anti-p21 antibody F-5 (sc-6246) were from Santa Cruz. Anti-p16 antibody was from BD PharMingen. The proteins were visualized by enhanced chemiluminescence according to the manufacturer's instructions (Amersham).

**Analysis of senescence.** SA-β-Gal staining was carried out using the Senescence Detection Kit (Oncogene) as instructed by the manufacturer. For each sample, at least 200 cells were counted in randomly chosen fields.

**Telomerase activity assays.** Total lysates of cells were subjected to the telomerase repeat amplification protocol using a TRAPEZE kit (Intergen) according to the manufacturer's instructions.

**Soft-agar colony formation assays.** Soft-agar growth assays were carried out as described previously.[19] At the time of plating in soft agar, cultures were trypsinized and counted, and $5 \times 10^3$ or $5 \times 10^4$ total cells were mixed with 1.5 mL of 0.35% Noble agar-DMEM (top layer) and then poured on top of 5 mL of solidified 0.7% Noble agar-DMEM (bottom layer) in 6-cm-diameter dishes. After 3 weeks, colonies were counted, and pictures were taken.

**Tumorigenicity assays.** A total of $1 \times 10^6$ cells were resuspended in 50 μL Matrigel solution (BD Matrigel Basement Membrane Matrix HC; BD Biosciences) and immediately injected subcutaneously into 8-week-old female nude mice (BALB/cAnNCrl-nu BR). 2-D tumor sizes were measured once a week. The tumor volume ($mm^3$) was calculated using the formula (length × width$^2$)/2.[21]

## Results

**Effect of HBx on cellular senescence of human primary cells.** During immortalization, human cells differ from rodent cells in the regulation of telomere length[22,23] and cell cycle checkpoints.[24,25] Human cells must bypass two barriers to become immortalized: replicative senescence and crisis. Replicative senescence is characterized by an irreversible growth arrest but continued metabolic activity.[26] Crisis is characterized by widespread cell death.[26,27] By the introduction of hTERT, human primary cells avoid these two barriers and can become immortalized.[28–30]

It is possible that HBx contributes to the immortalization process of human primary cells, but not to the cellular transformation process. If so, it may facilitate cellular transformation indirectly by overcoming two crises, M1 and M2. To study whether this does facilitate cellular transformation, it is best to use human primary hepatocytes as HBV is a hepatotropic virus. However, human primary hepatocytes are almost impossible to obtain for such an experimental approach. HBx exhibits its transactivation function not only in hepatoma cell lines but also in various carcinoma and sarcoma cell lines. Under these situations, we addressed whether HBx contributes to the immortalization of human primary fibroblasts, BJ cells and TIG3 cells that have been well studied for cellular senescence and immortalization. We used hTERT-introduced BJ and TIG3 cells for positive controls of immortal cells.

The human primary fibroblasts, BJ cells and TIG3 cells were infected with the HBx-expression retroviruses and cultured in the presence of the selection drug, blasticidin S. The drug-resistant polyclonal cells were selected and characterized. Three different constructs of HBx were used to map the responsible domain: full-length HBx (HBx-wt), HBx-D1, which lacks the N-terminal negative regulatory domain, and HBx-D5, which lacks the coactivation domain (Fig. 1a). First we examined HBx expression in the primary human fibroblasts. We found that full-length HBx and HBx-D5 were highly but equally expressed, whereas expression of HBx-D1 was very weak in the blasticidin S-selected clones (Fig. 1b). We hypothesized that HBx expression may confer an immortal phenotype, which could contribute to cellular transformation and tumorigenesis, but we observed that the BJ cells expressing HBx proteins stopped dividing at PD 69.6 ± 0.9 (errors ± SD) (HBx-wt), PD 66.6 ± 1.6 (HBx-D5), PD 66.1 ± 1.4 (HBx-D1) and PD 60.5 ± 0.6 (control cells) (Fig. 1c). TIG3 cells, another human fibroblast, expressing HBx proteins stopped dividing at PD 77.2 ± 1.1 (HBx-wt), PD 75.1 ± 0.8 (HBx-D5), PD 75.1 ± 0.1 (HBx-D1) and PD 75.4 ± 0.2 (control cells) (Fig. 1d). Although a very minor extended lifespan (2–4 PD) was observed with HBx-wt-expressing primary human fibroblasts, the HBx protein could not elicit immortalization. We examined whether the effect of HBx on delay of cellular senescence was correlated with putative augmentation of telomerase activity in HBx-introduced BJ and TIG3 cells (Fig. 1e) as activation of the hTERT promoter was observed in hepatoma cell lines that were transiently cotransfected with the HBx expression vector and luciferase reporter vector of the hTERT promoter (S. Murakami *et al.* unpublished data, 2005). Telomerase activity in the extracts of cells expressing HBx-wt or HBx-D1 was slightly higher than that of cells expressing empty vector or HBx-D5 in both kinds of cells (Fig. 1e), but we failed to detect an increase in hTERT protein expression (data not shown). Therefore, the relevance of the weak augmentation of telomerase activity in the HBx-expressing primary cells remains unclear.

**Effect of HBx on immortalized BJ-hTERT cells.** Next, we addressed whether HBx facilitates the cellular transformation process

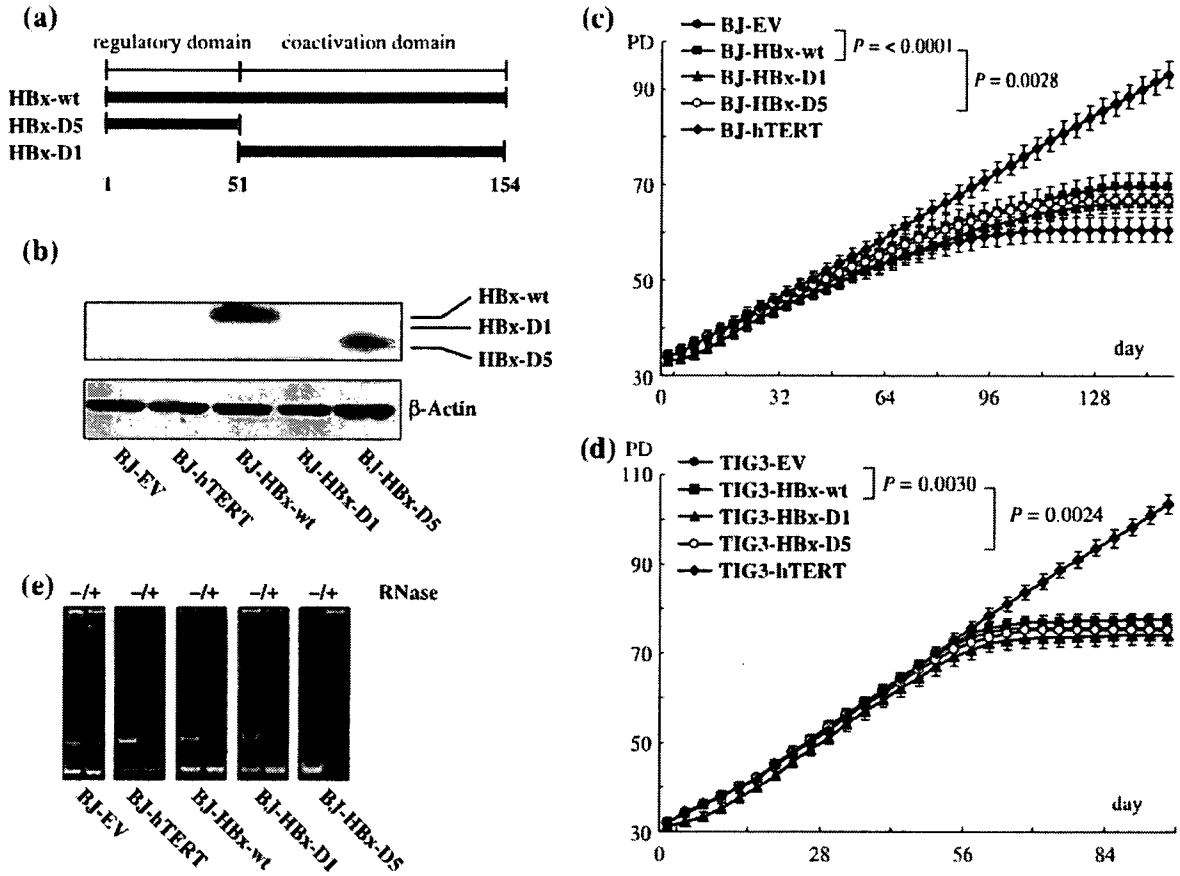


**Fig. 1.** Hepatitis B virus protein X (HBx) can not immortalize human primary cells, but weakly affects cellular senescence and telomerase activity. (a) Schematic representation of the HBx proteins.[5,8] The amino acids (aa) of full-length HBx (154 aa residues) and truncated HBx are shown. HBxD1 harbors the carboxy-terminal coactivation domain, spanning aa residues 51–154, whereas, HBxD5 harbors the amino-terminal negative regulatory domain, spanning aa residues 1–50. (b) Expression of HBx, HBx-D1 and HBx-D5 proteins in infected BJ cells. Total cell lysates of BJ cells infected with the empty vector (EV), human telomerase reverse transcriptase (hTERT), HBx, HBx-D1 and HBx-D5 expression retroviruses were fractionated by sodium dodecylsulfate–polyacrylamide gel electrophoresis and subjected to western blot analysis with anti-FLAG M2 antibody. (c) Effect of HBx on replicative senescence in BJ cells. BJ cells were infected with a control vector (filled circles) or hTERT (filled diamonds) and with a retrovirus encoding wild-type HBx (filled squares), HBx-D1 (filled triangles) or HBx-D5 (open circles). Cells infected with pBabe-puro- and pBabe-blast were selected with 1 μg/mL puromycin and 4 μg/mL blasticidin S, respectively. After 8 days of drug selection, triplicate samples of $1 \times 10^5$ cells were plated and grown under normal conditions (day 0). (d) Effect of HBx mutants on replicative senescence in TIG3 cells. Symbols are the same as in (c). (e) Telomerase activity in BJ cells as demonstrated by telomerase activity assay (TRAP). Total cell lysates (200 ng) prepared from BJ cells infected with control vector, hTERT, HBx, HBx-D1, and HBx-D5 were subjected to TRAP assay using a TRAPEZE kit (Intergen).

using human immortal cells. For this purpose, we used BJ-hTERT cells – these were BJ-derived cells immortalized by the introduction of hTERT, as characterized previously.[19] HBx-wt as well as its truncated mutants had no effect on cell proliferation, telomerase activity or cell transformation. Using the newly established TIG3-hTERT cells, we confirmed that the stable expression of HBx, XD1 or XD5 did not affect cell proliferation or cell transformation (data not shown). These results indicate the inability of HBx alone to transform these human immortalized cells.

**Ability of HBx to overcome H-RAS$^{V12}$-induced senescence in BJ cells immortalized by hTERT** Seeing as HBx did not exhibit the ability to immortalize primary human fibroblasts or to elicit transformation into hTERT-induced immortal primary human fibroblasts, we considered whether HBx functioned together with an oncogene and induced cell transformation. Senescence induced by active oncogene expression (OIS), such as oncogenic RAS, is one of the anticancer processes in which tumor suppressors and their related networks are involved, as demonstrated *in vitro* and recently also *in vivo*.[31,32] Overcoming OIS is critical for cellular transformation *in vitro* and cancerous cell proliferation *in vivo*.[31] Therefore, we addressed whether HBx has a collaborating role in transforming cells in the presence of oncogenic RAS or in overcoming RAS-induced senescence.

To examine the effect of HBx on RAS-induced senescence-like growth arrest, we introduced H-RAS$^{V12}$ into BJ-hTERT, BJ-hTERT-HBx-wt, BJ-hTERT-HBx-D1 and BJ-hTERT-HBx-D5 cells using a retrovirus (Fig. 2d). BJ-hTERT cells expressing H-RAS$^{V12}$ stopped proliferating within several days of RAS introduction. In contrast, BJ-hTERT cells expressing both H-RAS$^{V12}$ and HBx-wt (BJ-hTERT + H-RAS$^{V12}$ + HBx-wt) continued to proliferate to more than 80 PD (Fig. 2a). Although HBx-D1 also demonstrated the ability to overcome active RAS-induced senescence, HBx-D5 failed to overcome OIS (Fig. 2a). We also found that the growth rate of BJ-hTERT + H-RAS$^{V12}$ + HBx-wt cells was much higher than that of BJ-hTERT + H-RAS$^{V12}$ + HBx-D1 cells, probably reflecting the fact that some portion of the latter cells were positive for SA-β-gal (Fig. 2b,c). Consistent with this result, cells staining positive for SA-β-gal were significantly fewer in BJ-hTERT +



doi: 10.1111/j.1349-7006.2007.00579.x

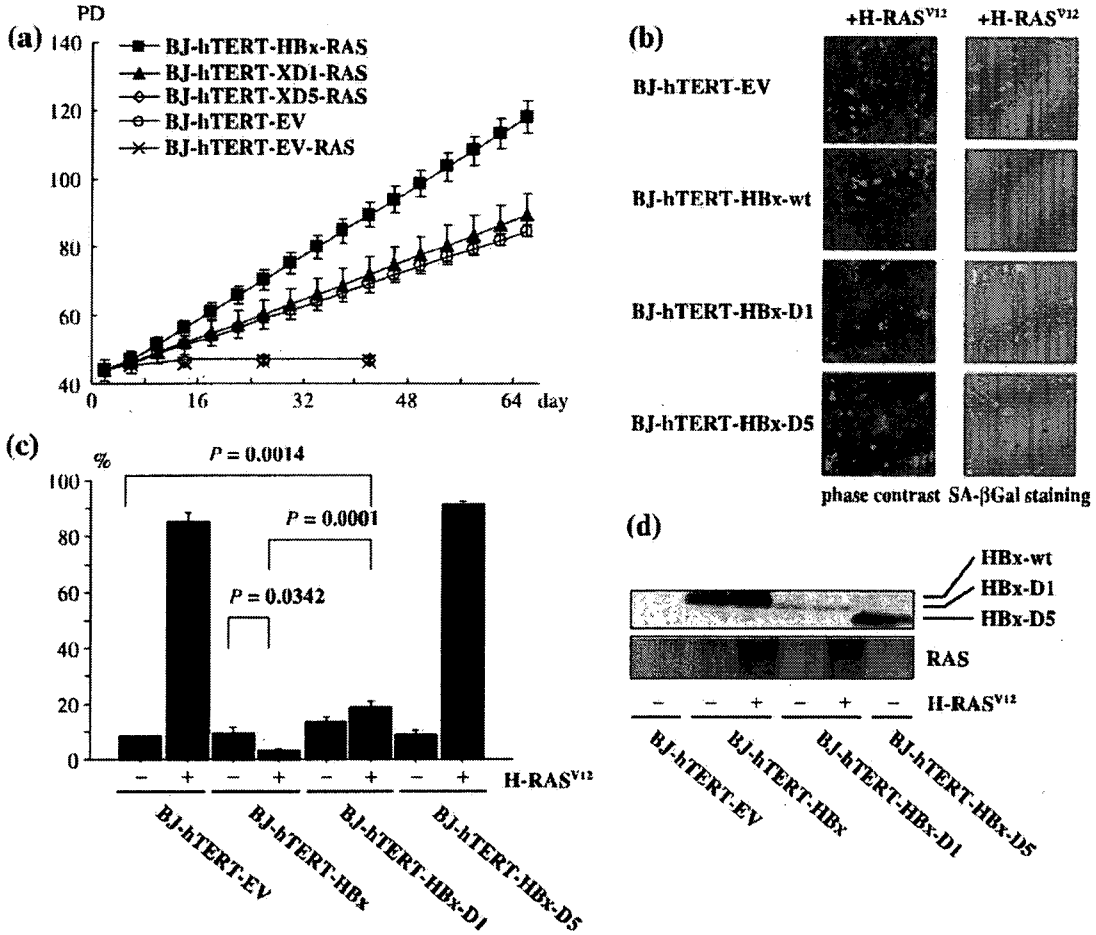


**Fig. 2.** Hepatitis B virus protein X (HBx) can overcome H-RAS$^{V12}$-induced cellular senescence of human immortalized cells. (a) Effect of HBx on H-RAS$^{V12}$ induced senescence. BJ-human telomerase reverse transcriptase (hTERT) cells (open circles) and H-RAS$^{V12}$-induced BJ-hTERT-HBx-wt (filled squares), BJ-hTERT-HBx-D1 (filled triangles), BJ-hTERT-HBx-D5 (filled diamonds) cells and BJ-hTERT-empty vector (EV) (cross) are shown. After 10 days of drug selection at population doubling (PD) 42, triplicate samples of $1 \times 10^5$ cells were plated and grown under normal conditions (day 0). (b) HBx overcomes H-RAS$^{V12}$-induced senescence of human immortalized cells. H-RAS$^{V12}$ and EV, full-length or truncated forms of HBx were introduced into BJ-hTERT cells. Left panel shows photographs 10 days after infection of the H-RAS$^{V12}$-expression retrovirus. Right panels show senescence-associated β-galactosidase (SA-β-Gal) staining 10 days after infection. (c) The percentage of cells positive for SA-β-Gal was determined in BJ cells stably expressing HBx-wt, HBx-D1, HBx-D5 or empty vector, with or without H-RAS$^{V12}$ on day 9 after infection. Bars = mean ± SD. (d) Western blot analysis of RAS-induced cells. Total cell lysates from BJ-hTERT cells stably expressing HBx-wt, HBx-D1, HBx-D5 or EV together with or without H-RAS$^{V12}$ were prepared and fractionated by sodium dodecylsulfate-polyacrylamide gel electrophoresis, then subjected to western blot analysis. HBx-wt, HBx-D1 and HBx-D5 were detected with anti-FLAG M2 antibody. RAS protein was detected with anti-RAS antibody.

H-RAS$^{V12}$ + HBx-wt than in BJ-hTERT + H-RAS$^{V12}$ + HBx-D1 (Fig. 2c). These results indicate that HBx-wt has the ability to overcome RAS-induced senescence. HBx-D1, the coactivator domain of HBx, seems to be indispensable and sufficient for overcoming RAS-induced senescence analyzed by the PD analysis, although HBx-D1 did not show the same ability as HBx-wt. The incomplete ability of HBx-D1 may be due to the low expression of HBx-D1 in the blastcidin S-selected clones in BJ-hTERT cells, as observed with the BJ cells (see Discussion).

**HBx protein is required for anchorage-independent growth and tumor formation in nude mouse in response to H-RAS$^{V12}$.** HBx can overcome RAS-induced senescence (examined by the PD analysis) and can indicate that HBx and RAS can induce cell transformation. Therefore, we examined whether BJ-hTERT + H-RAS$^{V12}$ + HBx-wt and BJ-hTERT + H-RAS$^{V12}$ + HBx-D1 cells can form colonies in soft agar. We found that BJ-hTERT + H-RAS$^{V12}$ + HBx-wt cells showed cell number-dependent formation of colonies, which were much smaller size than those of control cells, BJ-hTERT + H-RAS$^{V12}$ + SV40 LT + ST[20,33] (Fig. 3a,b). In contrast, BJ-hTERT + H-RAS$^{V12}$ + HBx-D1 cells could not form colonies in soft agar (Fig. 3a), although these cells overcame RAS-induced senescence. This result strongly suggests that HBx-D1 is not equivalent to HBx-wt in its ability to make colonies in soft agar.

Next we tested the tumor-forming ability of BJ-hTERT + H-RAS$^{V12}$ + HBx-wt or HBx-D1 cells in nude mice. BJ-hTERT + H-RAS$^{V12}$ + HBx-wt cells were found to form tumors in four of eight mice, although these tumors grew much more slowly and were much smaller than those formed by BJ-hTERT + H-RAS$^{V12}$ + SV40 LT + ST cells (eight of eight animals) (Fig. 3c). In contrast, BJ-hTERT + H-RAS$^{V12}$ + HBx-D1 cells did not generate tumors in nude mice (Fig. 3c), consistent with the results of the soft-agar assay. These results indicate that HBx contributes to cellular transformation by collaborating with active RAS in human immortalized cells. To our knowledge, this is the first report showing that HBx plays a critical role in

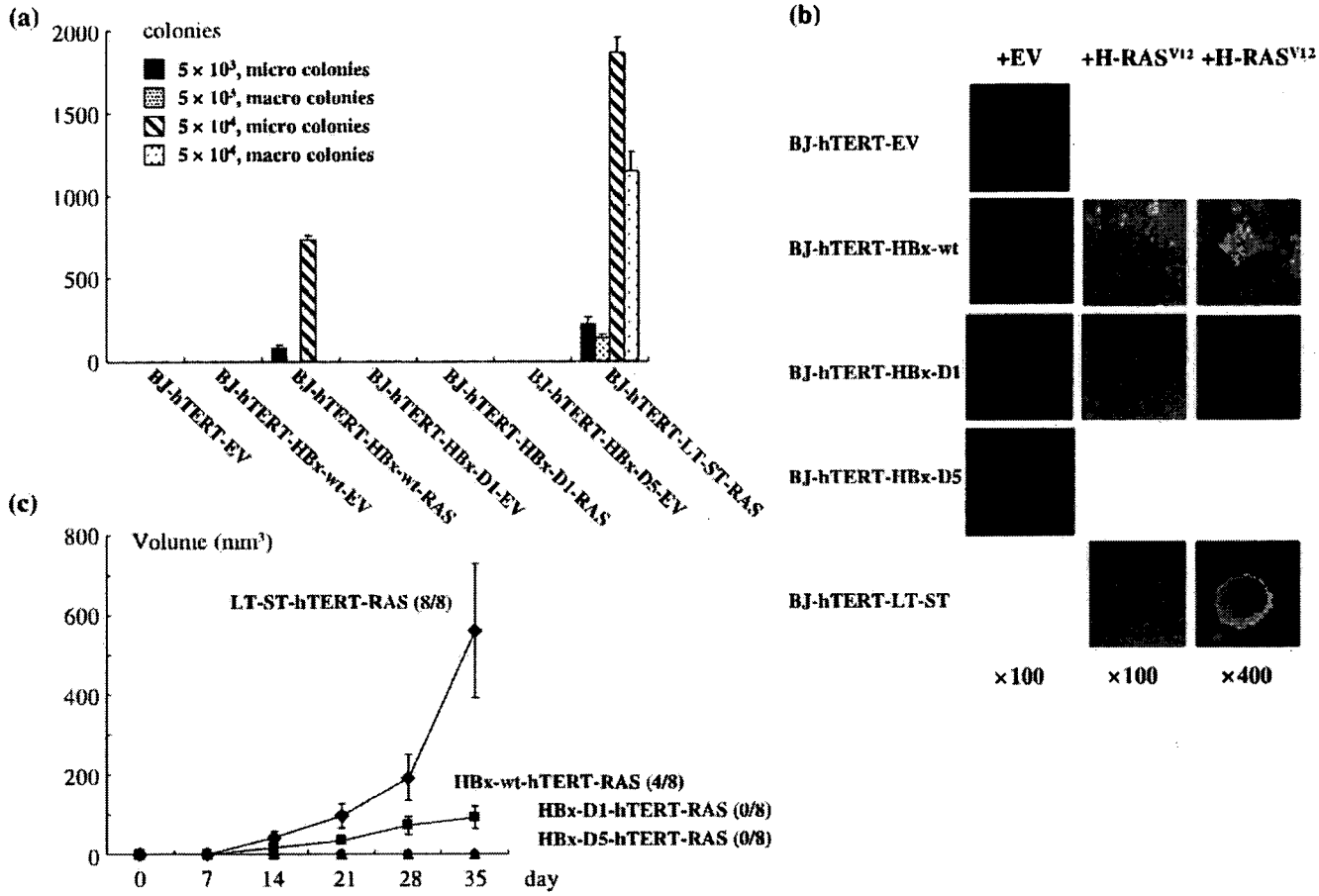


**Fig. 3** (a,b) Anchorage-independent growth in soft agar and (c) tumorigenicity and tumor-forming ability in nude mice of cells expressing hepatitis B virus X protein (HBx) and H-RAS$^{V12}$. (a) Soft-agar assays were carried out as described in Materials and Methods.[19] After 3 weeks, colonies were counted and pictures were taken. The colony-forming ability of BJ-human telomerase reverse transcriptase (hTERT) cells stably expressing wild-type or truncated HBx with or without H-RAS$^{V12}$ is indicated at the bottom. H-RAS$^{V12}$-introduced BJ-hTERT-LT-ST cells were the positive control. (b) Morphology of colonies in the soft-agar assay. Colonies were photographed 21 days after seeding. (c) Tumor formation in nude mice was carried out as described previously in Materials and Methods.[19,20] Tumor sizes were measured once a week. Each point on the graph represents the average volume of tumors. BJ-hTERT-LT-ST-RAS (filled diamonds), BJ-hTERT-HBx-RAS (filled squares), BJ-hTERT-HBx-D1 (filled circles), and BJ-hTERT (filled triangles) cells are shown. Error bars indicate the mean ± SD for each time point.

cellular transformation, collaborating with active RAS in human immortalized cells.

**Effects of HBx on p16 and p21 expression and the ability of HBx to overcome RAS-induced senescence.** Overexpression of RAS causes oncogene-induced premature senescence in normal human fibroblasts (Fig. 4c) and hTERT-immortalized human fibroblasts (Fig. 2a), but RAS failed to induce premature senescence in HBx-wt- or HBx-D1-introduced BJ-hTERT cells (Fig. 2a). We next examined the effect of stable expression of HBx in BJ cells with or without expression of hTERT, as interference with both the p53 and pRb pathways is necessary to avoid RAS-induced cellular senescence, in which p16 and p21 are the critical downstream effectors of pRb and p53, respectively. Expression of p16 and p21 was upregulated in HBx-wt- or HBx-D1-introduced BJ-hTERT cells; however, HBx-D5 has no ability to induce the expression of these genes. The presence of H-RAS$^{V12}$ resulted in downregulation of the augmented expression of p16 and p21 in HBx-wt- or HBx-D1-introduced BJ cells and BJ-hTERT cells (Fig. 4a,b). These results suggest that HBx can suppress expression of p53, p16 and p21 in H-RAS$^{V12}$-introduced cells, contributing to overcoming RAS-induced senescence. Next we examined whether HBx-wt and H-RAS$^{V12}$ not immortalized by hTERT were sufficient for cellular transformation. We introduced H-RAS$^{V12}$ into BJ-HBx-wt, BJ-HBx-D1 and BJ-HBx-D5 cells and analyzed them by PD analysis and soft-agar colony assay. In the PD analysis, H-RAS$^{V12}$-introduced BJ-HBx-wt and BJ-HBx-D1 cells did overcome RAS-induced cellular senescence but stopped cell division at PD 62, which is approximately the cellular senescence of BJ cells (Figs 1c,4c), whereas H-RAS$^{V12}$-introduced BJ-HBx-D5 did not overcome senescence and stopped cell division. These results suggest that HBx can overcome RAS-induced senescence but can not immortalize the cells (Fig. 4c). In the soft-agar colony formation assay, BJ-HBx-wt-H-RAS$^{V12}$ and BJ-HBx-D1-H-RAS$^{V12}$ could but BJ-HBx-D5-H-RAS$^{V12}$ could not form very tiny colonies, suggesting that HBx-wt and H-RAS$^{V12}$ in the absence of hTERT may enable the cells to proliferate in an anchorage-independent manner (data not shown).

As HBx-D1, which was very weakly expressed, exhibited almost the same ability as HBx-wt to upregulate the tumor suppressor genes and to overcome RAS-induced senescence in these cells, we wondered whether HBx-D1 missing the N-terminal domain may have some negative effect on cell proliferation. Because the transient expression level of HBx-D1 in BJ cells was similar to those in HepG2 cells, as reported previously



doi: 10.1111/j.1349-7006.2007.00579.x

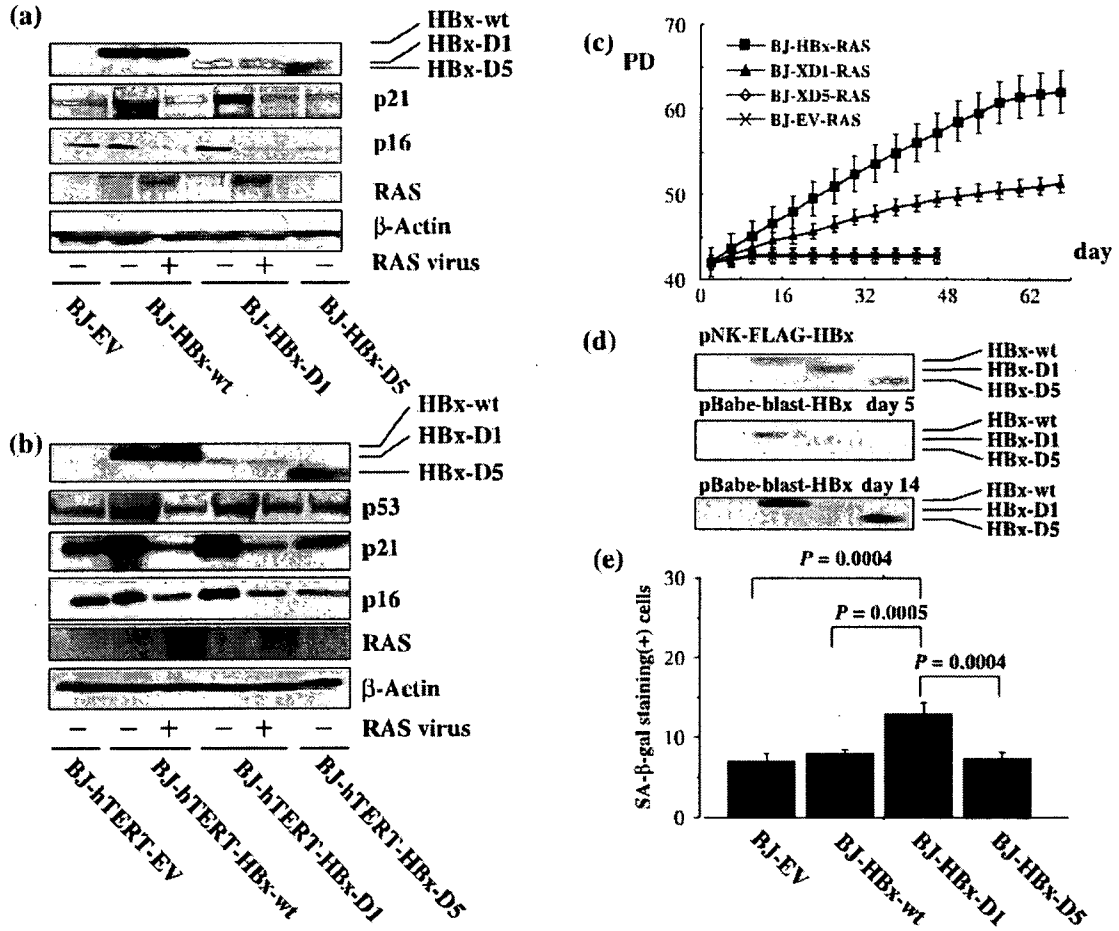


**Fig. 4.** Effect of hepatitis B virus X protein (HBx) on p16 and p21 expression and the ability of HBx to overcome H-RAS$^{V12}$-induced cellular senescence of human normal cells. Total cell lysates from BJ-human telomerase reverse transcriptase (hTERT) cells stably expressing HBx-wt, HBx-D1, HBx-D5 or empty vector together with or without H-RAS$^{V12}$ were prepared, and fractionated by sodium dodecylsulfate-polyacrylamide gel electrophoresis (SDS-PAGE), then subjected to western blot analysis. Expression of (a) p16 and p21 proteins and (b) p53, p16 and p21 proteins. (c) Effect of HBx on H-RAS$^{V12}$-induced senescence. Population doublings (PD) of H-RAS$^{V12}$-induced BJ-HBx-wt (filled squares), BJ-HBx-D1 (filled triangles), BJ-HBx-D5 (open diamonds) and BJ-EV (cross) cells are shown. After 10 days of drug selection, at PD 44, triplicate samples of $1 \times 10^5$ cells were plated and grown under normal conditions (day 0). (d) Expression of HBx, HBx-D1 and HBx-D5 proteins in infected BJ cells. Total cell lysates of BJ cells transfected with mammalian expression plasmids of FLAG-HBx-wt, FLAG-HBx-D1 and FLAG-HBx-D5 were fractionated by SDS-PAGE and subjected to western blot analysis with anti-FLAG M2 antibody (upper panel). Total cell lysates of BJ cells infected with the empty vector (EV), HBx-wt, HBx-D1 and HBx-D5 expression retroviruses were fractionated by SDS-PAGE and subjected to western blot analysis with anti-FLAG M2 antibody (middle and bottom panel). (e) The percentage of cells positive for senescence-associated β-galactosidase (SA-β-Gal) was determined in BJ cells stably expressing HBx-wt, HBx-D1, HBx-D5 or empty vector (EV) on day 40 after infection. Bars = mean ± SD.

(Fig. 4d),[8] it was not due to the construct design of the vector. The expression of HBx-D1 was slightly lower than those of HBx-wt and HBx-D5 on day 5 after selection, much lower on day 10 after selection (data not shown). On day 14 after selection, the expression of HBx-D1 reached the lowest level, and after day 14 that expression level was kept (Figs 1b,4d). HBx-D1-introduced BJ cells grew slower than HBx-wt- or HBx-D5-introduced BJ cells (data not shown) and contained more SA-β-Gal-positive cells during proliferation (Fig. 4e). These results suggest that cells expressing lower levels of HBx-D1 proliferated more than cells expressing higher levels of HBx-D1, due to some toxic or antiproliferative effect of the coactivation domain of HBx in the human primary cells (see Discussion).

**Important region of HBx for overcoming cellular senescence and anchorage-independent growth.** As HBx exhibited the ability to overcome active RAS-induced senescence, we next tried to identify the critical regions of HBx for overcoming cellular senescence. BJ-hTERT cells were infected with retroviruses expressing one of the clustered alanine-substituted mutants covering all parts of HBx,[34] and a series of cell clones stably expressing these HBx-cm mutants, BJ-hTERT-HBx-cm, was established (Fig. 5). H-RAS$^{V12}$ was then introduced into BJ-hTERT-HBx-cm1 to BJ-hTERT-HBx-cm21 cells and cell proliferation was examined. The regions covering HBx-cm8 to HBx-cm10, and those covering HBx-cm19 to HBx-cm21 were found to be not critical for overcoming active RAS-induced senescence and anchorage-independent growth as the BJ-hTERT-RAS clones expressing these HBx-cm mutants proliferated and formed colonies in soft agar, similar to BJ-hTERT-HBx-wt-H-RAS$^{V12}$ cells. The BJ-hTERT-RAS clones expressing HBx-cm1 to HBx-cm7, and those expressing HBx-cm14 to HBx-cm16, were like BJ-hTERT-HBx-D1-RAS, which can grow but at a much reduced rate compared with BJ-hTERT-HBx-RAS cells. The HBx regions covering HBx-cm11 to HBx-cm13, HBx-cm17

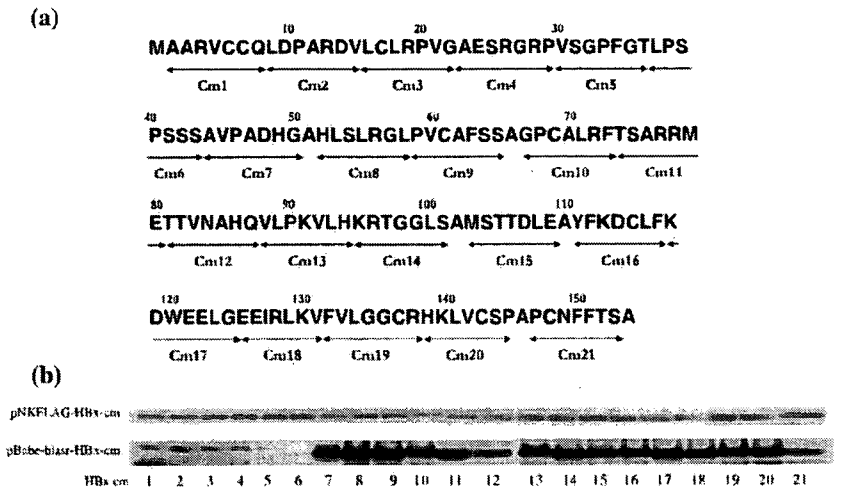


**Fig. 5.** Expression of hepatitis B virus X protein (HBx) library of clustered alanine substitution mutants in BJ-human telomerase reverse transcriptase (hTERT) cells. (a) Schematic representations of a series of clustered alanine substitution mutants (cm1 to cm21) of HBx. The amino acid locations of the clustered mutations are shown. (b) Detection of the mutated HBx proteins. Total cell lysates prepared from BJ-hTERT cells transfected with the mutant HBx expression vectors were fractionated by sodium dodecylsulfate–polyacrylamide gel electrophoresis and subjected to western blot analysis with anti-FLAG M2 antibody.

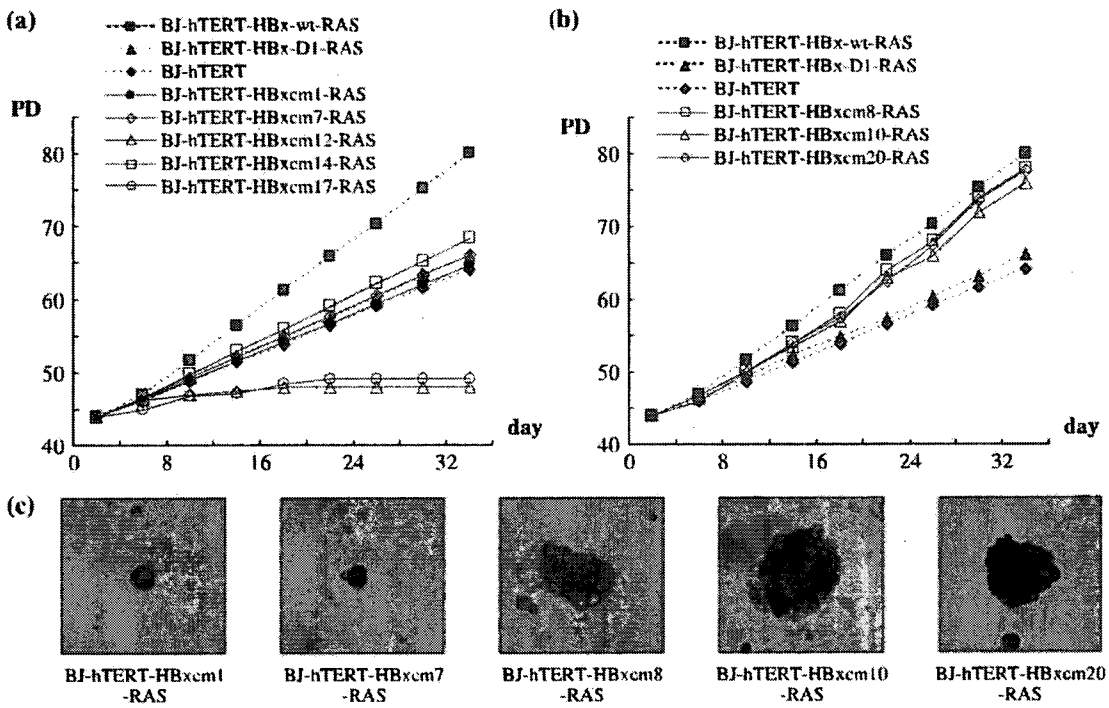


**Fig. 6.** Critical regions of hepatitis B virus X protein (HBx)-wt for tumorigenic function. (a) Effect of HBx-cm1–7 and HBx-cm11–18 failed to overcome H-RAS$^{V12}$-induced cellular senescence. Cell proliferation curves of several HBx-cm clones introduced with BJ-human telomerase reverse transcriptase (hTERT)-H-RAS$^{V12}$ in addition to those of BJ-hTERT cells (filled diamonds), H-RAS$^{V12}$-introduced BJ-hTERT-HBx-wt cells (filled squares) and BJ-hTERT-HBx-D1 cells (filled triangles) are shown. HBx-cm1, -cm7, -cm12, -cm14 and -cm17 were selected. HBx-cm1 (closed circles) and HBx-cm7 (open diamonds) represent HBx-cm1–7-introduced BJ-hTERT-H-RAS$^{V12}$ cells. HBx-cm12 (open triangles) represents HBx-cm11–13-introduced BJ-hTERT-H-RAS$^{V12}$ cells. HBx-cm14 (open squares) represents HBx-cm14–16-introduced BJ-hTERT-H-RAS$^{V12}$ cells. HBx-cm17 (open circles) represents HBx-cm17 and HBx-cm18-introduced BJ-hTERT-H-RAS$^{V12}$ cells. pBabe-puro-RAS-infected cells were selected with 1 μg/mL puromycin. After 10 days of drug selection at population doubling (PD) 44, triplicate samples of $1 \times 10^5$ cells were plated and grown under normal conditions. (b) Effect of HBx-cm8–10 and HBx-cm19–21 overcomes H-RAS$^{V12}$-induced cellular senescence. Cell proliferation curves of several HBx-cm clones introduced into BJ-hTERT-H-RAS$^{V12}$ in addition to those of BJ-hTERT cells (filled diamonds), H-RAS$^{V12}$-introduced BJ-hTERT-HBx-wt cells (filled square) and BJ-hTERT-HBx-D1 cells (filled triangles) are shown. HBx-cm8 (open squares) and HBx-cm10 (open triangles) represent HBx-cm8–10-introduced BJ-hTERT-H-RAS$^{V12}$ cells. HBx-cm20 (open diamonds) represents HBx-cm19–21-introduced BJ-hTERT-H-RAS$^{V12}$ cells.

and HBx-cm18 were found to be critical for overcoming active RAS-induced senescence as the BJ-hTERT-RAS clones expressing these HBx-cm mutants failed to proliferate, meaning that these had no ability to overcome active RAS-induced cellular senescence at all (Fig. 6) (Table 1). Among the BJ-hTERT-HBx-cm cells, expression levels of HBx-cm1 to HBx-cm6 were very weak, like that of HBx-D1. Furthermore, the protein bands of HBx-cm1 to HBx-cm5 migrated slightly slower than those of HBx-cm6 and the other HBx-cm mutants in the coactivation domain in SDS-PAGE analysis (see Discussion).



doi: 10.1111/j.1349-7006.2007.00579.x

**Table 1. Degree of proliferation of H-RAS$^{V12}$-introduced BJ-hTERT-HBx-cm cells**

| Cell type | Degree of proliferation |
|---|---|
| HBx-cm1[†] | +[‡] |
| HBx-cm2 | + |
| HBx-cm3 | + |
| HBx-cm4 | + |
| HBx-cm5 | + |
| HBx-cm6 | + |
| HBx-cm7 | + |
| HBx-cm8 | ++[§] |
| HBx-cm9 | ++ |
| HBx-cm10 | ++ |
| HBx-cm11 | – |
| HBx-cm12 | –[¶] |
| HBx-cm13 | – |
| HBx-cm14 | + |
| HBx-cm15 | + |
| HBx-cm16 | + |
| HBx-cm17 | – |
| HBx-cm18 | – |
| HBx-cm19 | ++ |
| HBx-cm20 | ++ |
| HBx-cm21 | ++ |

[†]HBx-cm1–21 in this table represent HBx-cm1–21-introduced BJ-hTERT-H-RAS$^{V12}$ cells. [‡]Same as BJ-hTERT-HBx-D1-H-RAS$^{V12}$ cells. [§]Same as BJ-hTERT-HBx-wt-H-RAS$^{V12}$ cells. [¶]Senescence.

## Discussion

Hepatitis B virus X protein has long been suspected to be positively involved in HBV-associated HCC, but its molecular role in hepatocarcinogenesis remains unclear. Although HBx is involved directly in the transformation of immortal rodent cells *in vitro* and in tumor formation in the livers of nude mice, the oncogenic activity of HBx itself remains to be elicited as the reproducibility of these experiments has been seriously controversial.[5] Furthermore, the positive role of HBx has not been addressed with human primary cells or human immortal cells. To our knowledge, our report is the first to show that HBx retains the ability to overcome RAS-induced senescence of immortalized human cells, although it is not sufficient for immortalizing human primary cells or transforming human immortal cells. hTERT-immortalized human cells stably expressing HBx-wt and RAS can form colonies in soft agar and tumors in nude mice in a cell-number-dependent manner. HBx can overcome RAS-induced senescence of BJ cells, but HBx-wt and active RAS could not immortalize the human fibroblasts. Although our findings are different to a report showing that HBx itself retains the transforming ability in NIH3T3 cells,[9] they are similar to results in rodent immortal embryonic fibroblast cells.[10]

To determine the region of HBx responsible for the ability to overcome RAS-induced senescence, we used two truncation mutants: HBx-D1 (aa 51–154), which exhibits transcriptional coactivation function and augments HBV transcription and replication,[8] and HBx-D5 (aa 1–50), which harbors the negative regulatory domain of transcriptional modulation.[6] When HBx-D1 and H-RAS$^{V12}$ were introduced into BJ-hTERT cells, HBx-D1 was similar to wild-type HBx in overcoming RAS-induced senescence in the PD analysis and in SA-β-gal staining. Therefore, HBx-D1 alone seems to be sufficient for overcoming active RAS-induced senescence and for anchorage-independent growth, but it is not sufficient for BJ-hTERT + H-RAS$^{V12}$ + HBx-D1 cells to form visible colonies in soft agar and tumors in nude mice. HBx alone may be sufficient for overcoming RAS-induced senescence, but hTERT is required for immortal proliferation of the transformed cells with H-RAS$^{V12}$ and HBx. As HBx-D1 exhibits a similar ability to HBx-wt in overcoming RAS-induced senescence and anchorage-independent growth, but not in immortalizing human fibroblasts, HBx-D1 may harbor all of the critical abilities of HBx. However, HBx-D1 is different from HBx-wt in the ability to form visible colonies in soft agar and to form tumors in nude mice.

The coactivation function was recently mapped by scanning a HBx library of clustered alanine substitution mutants (HBx-cm library), and two separate sequences in HBx-D1 were found to be critical.[8] Using the same HBx-cm library, we attempted to map the sequences critical for overcoming RAS-induced senescence. We have identified three different phenotypes among the HBx-cm mutants: those phenotypes are like HBx-wt, HBx-D1 and HBx-D5 (Fig. 6). HBx-cm mutations within the D5 region, cm1 to cm7, have the ability to partially overcome OIS, whereas those within the D1 region (cm8–10, cm14–16 and cm 19–21) fail to exhibit the overcoming ability. The HBx-D5 phenotype is even found among the HBx-cm mutants (cm13, cm17 and cm18) that are defective in the coactivation function.[8] These results indicate that the ability to fully overcome OIS requires two putative functions carried by the D1 and D5 regions of the HBx protein. Because HBx-D5 does not have a positive or negative effect on RAS-induced senescence (Figs 2,3,4c), the negative regulatory domain may be active only in full-length HBx. The very low expression of HBx-D1 in human primary cells and hTERT-immortalized cells may be due to the selection result of clones, reflecting that a high level of HBx-D1 protein was eliminated due to a toxic effect of the coactivation domain,[5] or due to deletion of the N-terminal domain that has some critical role in stabilizing HBx in the expression system. Both of these may actually occur. The former is supported by the enrichment of cells expressing HBx-D1 during the early stages of drug selection. The latter is highly possible as expression levels of HBx-cm1 to HBx-cm6 covering most of the N-terminal domain were very low, as for HBx-D1. Pang *et al.* recently reported a stabilization mechanism of HBx through direct interaction with Pin1,[35] which binds phosphorylated serine and the next proline. The target serine residue is within the N-terminal domain or within the region covered by HBx-cm6. Interestingly, the HBx-cm1 to HBx-cm5 bands migrated more slowly than the HBx-cm6 band (Fig. 5b), supporting the possibility that the N-terminal domain may be critical for Pin1 binding to stabilize HBx. One interesting possibility that remains to be tested is that activation of the degradation pathway of HBx causes the toxic effect on cell proliferation. This possibility may explain the low expression of HBx-D1 and the cm mutants in the N-terminal domain. In this context, it remains unclear at present the reason for the rather stable expression of two bands of HBx-cm7 that seem to confer the same phenotype as HBx-D1 in the characterization of the cells.

The region of D1 that is responsible for overcoming RAS-induced senescence should be defined. Because some HBx-cm mutants defective in coactivation function still exhibit the ability to overcome OIS, it seems that the coactivation function is dispensable for the role. More than a dozen host factors have been reported to interact directly with the HBx-D1 region, including p53,[36,37] Smad4,[38] DDB1,[39,40] and two core subunits of the proteasome.[5] It is especially important to determine whether the binding of HBx to p53 is responsible for the ability to overcome RAS-induced senescence, as the direct binding of p53 to HBx was found to suppress p53-dependent gene activation.[5,37]

Although we have shown here that the D5 region of HBx has an indispensable biological role in anchorage-independent cell growth, the critical role of the D5 region in overcoming OIS remains obscure. The ability of the D5 region in full-length HBx

to support anchorage-independent growth will provide a good experimental system for revealing the function of the negative regulatory domain of HBx, as no host factor has been reported to interact specifically with the D5 region.

Our results clearly indicate that HBx retains the ability to overcome RAS-induced senescence in human cells immortalized by hTERT, although HBx alone could neither immortalize nor transform human cells. The ability of HBx to collaborate with active RAS in cell transformation may explain its role in hepatocellular carcinogenesis. Our findings, however, were obtained using an experimental model with immortalized cells derived from human fibroblasts. Our results may not reflect the role of HBx in HBV-infected liver, as overcoming the processes of OIS seems to vary with tissue and tumor type.[41] The role of HBx should therefore be addressed using human hepatocytes and immortalized human hepatocytes. The former, however, are quite difficult to obtain whereas the latter are available at present. It had been immortalized by introducing the other viral oncogene SV LT.[42,43]

## Acknowledgments

We thank K. Masutomi and W. C. Hahn for kindly providing the retroviral vectors and human immortal cell lines, T. B. S. Yen (UCSF, USA) and H. Tang (Sichuan University, China) and the members of the Division for critical discussions, and Ms Yasukawa and Ms Kuwabara for excellent technical assistance. This work was supported in part by a Grant-in-aid for Scientific Research and Development (B) (1790031) and a Grant-in-aid for Scientific Research on Priority Areas (C) (12213050 and 17013035) from the Ministry of Education, Culture, Sports, and Technology.

## References

1 Seeger C, Mason WS. Hepatitis B virus biology. *Microbiol Mol Biol Rev* 2000; 64: 51–68.
2 Nassal M, Schaller H. Hepatitis B virus replication. *Trends Microbiol* 1993; 1: 221–8.
3 Arbuthnot P, Kew M. Hepatitis B virus and hepatocellular carcinoma. *Int J Exp Pathol* 2001; 82: 77–100.
4 Murakami S. Hepatitis B virus X protein: structure, function and biology. *Intervirology* 1999; 42: 81–99.
5 Murakami S. Hepatitis B virus X protein: a multifunctional viral regulator. *J Gastroenterol* 2001; 36: 651–60.
6 Murakami S, Cheong JH, Kaneko S. Human hepatitis virus X gene encodes a regulatory domain that represses transactivation of X protein. *J Biol Chem* 1994; 269: 15 118–23.
7 Lin Y, Tang H, Nomura T *et al.* The hepatitis B virus X protein is a co-activator of activated transcription that modulates the transcription machinery and distal binding activators. *J Biol Chem* 1998; 273: 27 097–103.
8 Tang H, Delgermaa L, Huang F *et al.* The transcriptional transactivation function of HBx protein is important for its augmentation role in hepatitis B virus replication. *J Virol* 2005; 79: 5548–56.
9 Shirakata Y, Kawada M, Fujiki Y *et al.* The X gene of hepatitis B virus induced growth stimulation and tumorigenic transformation of mouse NIH3T3 cells. *Jpn J Cancer Res* 1989; 80: 617–21.
10 Kim YC, Song KS, Yoon G *et al.* Activated ras oncogene collaborates with HBx gene of hepatitis B virus to transform cells by suppressing HBx-mediated apoptosis. *Oncogene* 2001; 20: 16–23.
11 Kim CM, Koike K, Saito I, Miyamura T, Jay G. HBx gene of hepatitis B virus induces liver cancer in transgenic mice. *Nature* 1991; 351: 317–20.
12 Yu DY, Moon HB, Son JK *et al.* Incidence of hepatocellular carcinoma in transgenic mice expressing the hepatitis B virus X-protein. *J Hepatol* 1999; 31: 123–32.
13 Gottlob K, Pagano S, Levrero M, Graessmann A. Hepatitis B virus X protein transcription activation domains are neither required nor sufficient for cell transformation. *Cancer Res* 1998; 58: 3566–70.
14 Slagle BL, Lee TH, Medina D, Finegold MJ, Butel JS. Increased sensitivity to the hepatocarcinogen diethylnitrosamine in transgenic mice carrying the hepatitis B virus X gene. *Mol Carcinog* 1996; 15: 261–9.
15 Terradillos O, Billet O, Renard CA *et al.* The hepatitis B virus X gene potentiates c-myc-induced liver oncogenesis in transgenic mice. *Oncogene* 1997; 14: 395–404.
16 Artandi SE, DePinho RA. Mice without telomerase: what can they teach us about human cancer? *Nat Med* 2000; 6: 852–5.
17 Balmain A, Harris CC. Carcinogenesis in mouse and human cells: parallels and paradoxes. *Carcinogenesis* 2000; 21: 371–7.
18 Rangarajan A, Hong SJ, Gifford A, Weinberg RA. Species- and cell type-specific requirements for cellular transformation. *Cancer Cell* 2004; 6: 171–83.
19 Hahn WC, Counter CM, Lundberg AS, Beijersbergen RL, Brooks MW, Weinberg RA. Creation of human tumour cells with defined genetic elements. *Nature* 1999; 400: 464–8.
20 Wei W, Jobling WA, Chen W, Hahn WC, Sedivy JM. Abolition of cyclin-dependent kinase inhibitor p16Ink4a and p21Cip1/Waf1 functions permits Ras-induced anchorage-independent growth in telomerase-immortalized human fibroblasts. *Mol Cell Biol* 2003; 23: 2859–70.
21 Akagi T, Sasai K, Hanafusa H. Refractory nature of normal human diploid fibroblasts with respect to oncogene-mediated transformation. *Proc Natl Acad Sci USA* 2003; 100: 13 567–72.
22 Greenberg RA, Allsopp RC, Chin L, Morin GB, DePinho RA. Expression of mouse telomerase reverse transcriptase during development, differentiation and proliferation. *Oncogene* 1998; 16: 1723–30.
23 Newbold RF. Genetic control of telomerase and replicative senescence in human and rodent cells. *Ciba Found Symp* 1997; 211: 177–89.
24 Harvey M, Sands AT, Weiss RS. *et al. In vitro* growth characteristics of embryo fibroblasts isolated from p53-deficient mice. *Oncogene* 1993; 8: 2457–67.
25 Kamijo T, Zindy F, Roussel MF. *et al.* Tumor suppression at the mouse INK4a locus mediated by the alternative reading frame product p19ARF. *Cell* 1997; 91: 649–59.
26 Sedivy JM. Can ends justify the means? Telomeres and the mechanisms of replicative senescence and immortalization in mammalian cells. *Proc Natl Acad Sci USA* 1998; 95: 9078–81.
27 Shay JW, Wright WE, Werbin H. Defining the molecular mechanisms of human cell immortalization. *Biochim Biophys Acta* 1991; 1072: 1–7.
28 Bodnar AG, Ouellette M, Frolkis M *et al.* Extension of life-span by introduction of telomerase into normal human cells. *Science* 1998; 279: 349–52.
29 Halvorsen TL, Leibowitz G, Levine F. Telomerase activity is sufficient to allow transformed cells to escape from crisis. *Mol Cell Biol* 1999; 19: 1864–70.
30 Hahn WC. Role of telomeres and telomerase in the pathogenesis of human cancer. *J Clin Oncol* 2003; 21: 2034–43.
31 Sharpless NE, DePinho RA. Cancer: crime and punishment. *Nature* 2005; 436: 636–7.
32 Braig M, Lee S, Loddenkemper C *et al.* Oncogene-induced senescence as an initial barrier in lymphoma development. *Nature* 2005; 436: 660–5.
33 Hahn WC, Dessain SK, Brooks MW *et al.* Enumeration of the simian virus 40 early region elements necessary for human cell transformation. *Mol Cell Biol* 2002; 22: 2111–23.
34 Tang H, Oishi N, Kaneko S, Murakami S. Molecular functions and biological roles of hepatitis B virus X protein. *Cancer Sci* 2006; 97: 977–83.
35 Pang R, Lee TK, Poon RT *et al.* Pin1 interacts with a specific serine-proline motif of hepatitis B virus X-protein to enhance hepatocarcinogenesis. *Gastroenterology* 2007; 132: 1088–1103.
36 Elmore LW, Hancock AR, Chang SF *et al.* Hepatitis B virus X protein and p53 tumor suppressor interactions in the modulation of apoptosis. *Proc Natl Acad Sci USA* 1997; 94: 14 707–12.
37 Lin Y, Nomura T, Yamashita T, Dorjsuren D, Tang H, Murakami S. The transactivation and p53-interacting functions of hepatitis B virus X protein are mutually interfering but distinct. *Cancer Res* 1997; 57: 5137–42.
38 Lee DK, Park SH, Yi Y *et al.* The hepatitis B virus encoded oncoprotein pX amplifies TGF-beta family signaling through direct interaction with Smad4: potential mechanism of hepatitis B virus-induced liver fibrosis. *Genes Dev* 2001; 15: 455–66.
39 Lee TH, Elledge SJ, Butel JS. Hepatitis B virus X protein interacts with a probable cellular DNA repair protein. *J Virol* 1995; 69: 1107–14.
40 Leupin O, Bontron S, Schaeffer C, Strubin M. Hepatitis B virus X protein stimulates viral genome replication via a DDB1-dependent pathway distinct from that leading to cell death. *J Virol* 2005; 79: 4238–45.
41 DePinho RA. The age of cancer. *Nature* 2000; 408: 248–54.
42 Kobayashi N, Noguchi H, Watanabe T *et al.* A new approach to develop a biohybrid artificial liver using a tightly regulated human hepatocyte cell line. *Hum Cell* 2000; 13: 229–35.
43 Kobayashi N, Miyazaki M, Fukaya K *et al.* Treatment of surgically induced acute liver failure with transplantation of highly differentiated immortalized human hepatocytes. *Cell Transplant* 2000; 9: 733–5.



doi: 10.1111/j.1349-7006.2007.00579.x

American Journal of Gastroenterology
© 2007 by Am. Coll. of Gastroenterology
Published by Blackwell Publishing

ISSN 0002-9270
doi: 10.1111/j.1572-0241.2007.01354.x

# Impact of Diabetes on Recurrence of Hepatocellular Carcinoma after Surgical Treatment in Patients With Viral Hepatitis

Takuya Komura, M.D.,[1] Eishiro Mizukoshi, M.D.,[1] Yuki Kita, M.D.,[2] Masaru Sakurai, M.D.,[2] Yoshiko Takata, M.D.,[1] Kuniaki Arai, M.D.,[1] Tatsuya Yamashita, M.D.,[1] Tetsuo Ohta, M.D.,[3] Koichi Shimizu, M.D.,[3] Yasunari Nakamoto, M.D.,[1] Masao Honda, M.D.,[1] Toshinari Takamura, M.D.,[2] and Shuichi Kaneko, M.D.[1]

[1]*Department of Gastroenterology,* [2]*Department of Diabetes and Digestive Disease, and* [3]*Department of Gastroenterologic Surgery, Graduate School of Medicine, Kanazawa University, Kanazawa, Ishikawa, Japan*

**OBJECTIVES:** Consensus has been reached that diabetes is a risk factor for development of HCC, but the impact on postoperative recurrence is still controversial. To clarify this point, we analyzed the relationship of postoperative recurrence rate of HCC and coexistence of diabetes in the patients with viral hepatitis.

**METHODS:** A total of 90 patients who had undergone curative resection for HCC were analyzed. They were divided into two groups with and without diabetes, and the recurrence-free survival rates after surgical treatment and the factors contributing to recurrence were examined.

**RESULTS:** Kaplan-Meier survival analysis showed the recurrence-free survival rates in the diabetic group were significantly lower than those in the nondiabetic group ($P = 0.005$) and overall survival rates in the diabetic group were significantly lower than those in the nondiabetic group ($P = 0.005$). These results were emphasized in the analysis of patients infected with hepatitis C virus. Univariate and multivariate analyses showed diabetes was a significant factor contributing to HCC recurrence after treatment. Furthermore, multivariate analysis in HCC patients with diabetes showed Child-Pugh classification B ($P = 0.001$) and insulin therapy ($P = 0.049$) were significant factors contributing to HCC recurrence after treatment.

**CONCLUSIONS:** The results of the present study suggest that diabetes is a risk factor for the recurrence of HCV-related HCC and decreases the overall survival rates after surgical treatment. HCV-related HCC patients with diabetes should be closely followed for postoperative recurrence.

(Am J Gastroenterol 2007;102:1939-1946)

## INTRODUCTION

Hepatocellular carcinoma (HCC) is the fifth most frequent malignant neoplasm in the world (1), and its prevalence is particularly high in Asia and Africa. The recent increase in its prevalence has attracted the attention of researchers (2, 3). Surgical therapy provides complete cure for HCC, but the indication is limited to a relatively small number of patients. Recent remarkable advances in diagnostic imaging techniques and systematic hepatectomy have been improving the prognosis of patients with HCC, but these techniques have not provided satisfactory results (4, 5), because of a high post-treatment recurrence rate characterizing HCC. Previous studies have noted that factors contributing to recurrence include gender, alcohol consumption, hepatitis C virus (HCV) infection, hepatic reserve, liver fibrosis degree, tumor size, tumor differentiation degree, vascular factor, and alpha-fetoprotein (AFP) level (6–9).

On the other hand, recent studies have reported that coexistence of diabetes is a risk factor for the progression of liver fibrosis and the development of HCC in chronic hepatitis C (10, 11). These reports suggest that coexistence of diabetes is also involved in the high postoperative recurrence rate of HCC. However, it is controversial whether diabetes is an independent risk factor for the post-treatment recurrence of HCC. Ikeda *et al.* (12) reported that diabetes was a risk factor for the recurrence of HCC after surgical treatment, but Poon *et al.* (13) and Toyoda *et al.* (14) reported that this was not the case. The discrepancy among these reports is probably due in part to the difference in the etiology of liver disease in the patients studied.

In this study, to clarify the controversial point about diabetes and HCC recurrence, we examined the impact of diabetes on the postoperative recurrence of HCC in 90 patients who had undergone curative resection for HCC. In addition, we classified the HCC patients into groups of hepatitis B

virus (HBV)- and HCV-related HCC patients, and performed a close analysis of the impact of diabetes on the postoperative recurrence of HCC in each group.

## PATIENTS AND METHODS

### *Patients*

A total of 150 patients were diagnosed with primary HCC and underwent surgical treatment in Kanazawa University Hospital between June 1987 and May 2004. Of these patients, 90 were analyzed who had HBV or HCV infection and underwent curative resection.

HCCs were detected by imaging modalities such as ultrasound scan, dynamic CT scan, MR imaging, and abdominal arteriography. The diagnosis of HCC was made by typical hypervascular tumor staining on angiography in addition to using typical findings, which showed hyperattenuation areas in the early phase and hypoattenuation in the late phase on dynamic CT (15).

All resected tumors were examined pathologically for the degree of differentiation of HCC, vascular invasion, and persistence of tumor in the surgical stump. Pathological degree of differentiation of HCC was assessed according to the general rules for the clinical and pathologic study of primary liver cancer (16).

### *Treatment and Follow-Up*

In selecting surgery as a treatment option for HCC, we considered the following criteria: (a) good general condition of the patient whose Karnofsky performance status was over 80, (b) primary HCC, (c) Child-Pugh classification A or B, (d) the number of HCC was solitary and no CT, MRI, or angiographic evidence of vascular invasion or distant metastasis. Curative resection was defined as complete excision of the tumor with tumor-free surgical margins and no local recurrence at the surgical margin within 6 months after surgery.

Patients were followed postoperatively on an outpatient basis by abdominal ultrasound, dynamic CT, or MRI at 3-month intervals for at least 60 months. Recurrence was diagnosed by dynamic CT or MRI, and the date of recurrence was defined as the date of examination when the recurrence of HCC was noted. In patients with recurrent HCC, the recurrence-free period was defined as the time between the date of surgery and the date of recurrence. We confirmed the date of the patient's last visit to our hospital and checked the status of HCC using each patient's medical record.

### *Laboratory and Virologic Testing*

Blood samples were tested for hepatitis B surface antigen (HBs-Ag) and hepatitis C virus antibody (HCV-Ab) by commercial immunoassays (Fuji Rebio, Tokyo, Japan). Serum AFP level was measured by enzyme immunoassay (AxSYM AFP, Abbott Japan, Tokyo, Japan). Diabetes was diagnosed according to the American Diabetes Association criteria for type II diabetes (17) and the severity of liver disease (stage of fibrosis) was evaluated according to the criteria of Desmet *et al.* (18).

### *Statistical Analysis*

Between-group differences were assessed by univariate analysis with Student's $t$-test for numerical data and the $\chi 2$ test with Yates' correction (or Fisher's exact test where appropriate) for nominal data. Overall survival and recurrence-free survival was examined using the method of Kaplan-Meier, and differences were assessed by the log-rank test. Impact factors for the recurrence of HCC after hepatic resection were analyzed by univariate and multivariate analysis using Cox proportional hazards model. Seventeen variables were analyzed, consisting of age, gender, etiology, body mass index (BMI), prevalence of alcohol abuse, diabetes, hemoglobin A1c (HbA1c), liver fibrosis degree, Child-Pugh classification, platelet count, alanine aminotransferase (ALT), T-bil, Alb, AFP, tumor size, tumor differentiation degree, and the presence of vascular invasion. $P < 0.05$ was considered statistically significant.

## RESULTS

### *Comparison of Baseline Characteristics*

Of the 90 patients (75 men and 15 women, with a mean age of 61.0 yr) who were followed and analyzed, 30 were diagnosed as having coexistence of diabetes, and 60 had no diabetes. The characteristics of the patients in both groups

**Table 1.** Characteristics of Patients

| Characteristic | Patients With Diabetes (N = 30) | Patients Without Diabetes (N = 60) | *P* Value |
|---|---|---|---|
| Median age (yr) | 62.0 | 60.6 | 0.453 |
| Gender (male/female) | 24/6 | 51/9 | 0.560 |
| Etiology (HBV/HCV/HBV + HCV) | 8/22/0 | 17/40/3 | 0.438 |
| Body mass index (kg/m$^2$) | 23.5 | 22.73 | 0.316 |
| Alcohol abuse (+/−) | 13/17 | 27/33 | 0.881 |
| HbA1c (%) | 6.4 | 4.8 | <0.001 |
| HOMA-IR | 4.1 | 3.3 | 0.399 |
| Platelet count (× 10$^4$/μL) | 12.2 | 13.5 | 0.284 |
| ALT (IU/L) | 69.8 | 56.4 | 0.318 |
| Total bilirubin (mg/dL) | 0.9 | 0.8 | 0.510 |
| Albumin (g/dL) | 4.1 | 4.2 | 0.341 |
| AFP (ng/mL) | 417 | 395 | 0.931 |
| Fibrosis (F1/F2/F3/F4) | 0/4/4/22 | 4/5/5/46 | 0.732 |
| Inflammatory grading (A1/A2/A3) | 11/17/2 | 24/33/3 | 0.385 |
| Child-Pugh grade (A/B/C) | 24/6/0 | 53/7/0 | 0.294 |
| Tumor size (mm) | 34.3 | 29.8 | 0.359 |
| Diff. degree (wel/mod/por)* | 11/12/7 | 20/19/21 | 0.264 |
| Vascular invasion (+/−) | 11/19 | 20/40 | 0.757 |
| Date of operation (1987–1995/1995–2000/2001–2004) | 8/14/8 | 13/30/17 | 0.538 |

*Histological degree of HCC: wel = well differentiated; mod = moderately differentiated; por = poorly differentiated.

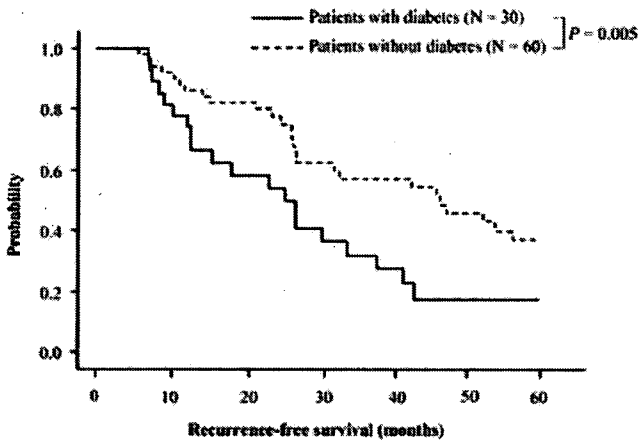


**Figure 1.** Kaplan-Meier curves for recurrence-free survival in the groups of patients with and without diabetes.

are shown in Table 1. No significant differences were noted between the two groups in age, gender, HBV or HCV infection rate, BMI, or prevalence of alcohol abuse. HbA1c was significantly higher, at 6.4%, in the diabetic group than in the nondiabetic group with an HbA1c of 4.8% ($P < 0.001$). There were no significant differences in platelet count, ALT, T-bil, Alb, AFP, or Child-Pugh classification between the two groups. In addition, no significant differences were observed in the liver fibrosis degree, or in the size, degree of differentiation, and presence of microscopic vascular invasion of resected HCC. Homeostasis model assessment-insulin resistance (HOMA-IR) of the patients with diabetes, which was high compared with that of Japanese healthy subjects (19), was higher than that of the patients without diabetes, although it was not statistically significant.

### *Impact of Diabetes on Recurrence After Surgical Treatment of HCC*

Next, the diabetic and nondiabetic groups were compared for the rate of HCC recurrence after surgical treatment. HCC recurred after surgical treatment in 49 patients, consisting of 22 diabetic patients (73.3%) and 27 nondiabetic patients (45.0%). The mean time to recurrence was 32.8 months (range 8–60 months) and the median time to recurrence was 29.4 months.

Figure 1 shows the Kaplan-Meier curves for recurrence-free survival of the patients with and without diabetes. The recurrence-free survival rates 1, 2, 3, 4, and 5 yr after surgical treatment were 77.8%, 55.6%, 36.0%, 16.7%, and 16.7%, respectively, in the diabetic patient group, and 89.5%, 80.4%, 56.8%, 45.0%, and 36.6%, respectively, in the nondiabetic patient group; all rates except 1 yr were significantly lower in the diabetic patient group ($P = 0.155$, $P = 0.010$, $P = 0.009$, $P = 0.002$, and $P = 0.005$).

To further examine the degree of contribution of diabetes to the postoperative recurrence of HCC, we performed univariate and multivariate analysis. Univariate analysis identified the following variables as factors significantly contributing to HCC recurrence after surgical treatment: presence of diabetes ($P = 0.003$), high HbA1c level ($P < 0.001$), and Child-Pugh classification B against A ($P < 0.001$) (Table 2). When we conducted multivariate analysis, we chose variables that had already pointed out a risk factor for HCC recurrence and the $P$ value was lower than 0.1 in univariate analysis. As a result, multivariate analysis of these variables showed that the presence of diabetes (risk 2.9, 95% CI 1.5–5.4, $P < 0.001$) and Child-Pugh classification B against A (risk 3.6, 95% CI 1.7–7.7, $P = 0.001$) were significant factors contributing to HCC recurrence after surgical treatment (Table 3).

**Table 2.** Univariate Proportional Hazard Model for Recurrence of HCC After Surgical Treatment

| Variable | Hazard Ratio | 95% CI | $P$ Value |
|---|---|---|---|
| Age (yr) | 1.0 | 1.0–1.1 | 0.258 |
| Gender (male) | 0.5 | 0.3–1.1 | 0.104 |
| Etiology (HCV) | 1.0 | 0.5–1.8 | 0.965 |
| Body mass index (>25 kg/m$^2$) | 1.2 | 0.6–2.3 | 0.554 |
| Alcohol abuse (+) | 1.1 | 0.7–2.0 | 0.644 |
| Diabetes (+) | 2.4 | 1.3–4.2 | 0.003 |
| HbA1c (%) | 1.5 | 1.2–1.9 | <0.001 |
| Fibrosis (F4) | 1.4 | 0.7–3.1 | 0.349 |
| Child-Pugh grade (B) | 3.1 | 1.6–6.0 | <0.001 |
| Platelet count ($\times 10^4/\mu$L) | 1.0 | 0.9–1.0 | 0.465 |
| ALT (IU/L) | 1.0 | 1.0–1.1 | 0.717 |
| Total bilirubin (mg/dL) | 1.4 | 0.6–3.6 | 0.451 |
| Albumin (g/dL) | 1.4 | 0.8–2.4 | 0.225 |
| AFP (>200 ng/mL) | 1.0 | 0.5–1.8 | 0.906 |
| Tumor size (>50 mm) | 1.5 | 0.7–1.2 | 0.213 |
| Diff. degree (P) | 1.1 | 0.6–2.1 | 0.675 |
| Vascular invasion (+) | 1.2 | 0.4–1.7 | 0.490 |

### *Impact of Diabetes on Prognosis After Surgical Treatment of HCC*

To examine the impact of diabetes on prognosis of HCC patients, we analyzed the overall survival rates after surgical treatment. Figure 2 shows the Kaplan-Meier curves for overall survival of the patients with and without diabetes after surgical treatment of HCC. The overall survival rates 1, 2, 3, 4, and 5 yr after surgical treatment were 100%, 88.9%, 75.0%, 63.6%, and 45.5%, respectively, in the diabetic patient group, and 100%, 98.1%, 88.9%, 85.7%, and 76.3%, respectively, in the nondiabetic patient group; the rates of more than 3 yr were significantly lower in the diabetic patient group ($P = 1.000$, $P = 0.073$, $P = 0.028$, $P = 0.039$, and $P = 0.005$).

**Table 3.** Multivariate Proportional Hazard Model for Recurrence of HCC After Surgical Treatment

| Variable | Hazard Ratio | 95% CI | $P$ Value |
|---|---|---|---|
| Diabetes | 2.9 | 1.5–5.5 | <0.001 |
| Fibrosis (F4) | 1.9 | 0.8–4.5 | 0.148 |
| Child-Pugh grade (B) | 3.6 | 1.7–7.7 | 0.001 |
| AFP(>200 ng/mL) | 0.7 | 0.3–1.5 | 0.390 |
| Diff. degree (P) | 0.9 | 0.5–1.8 | 0.776 |
| Vascular invasion (+) | 2.0 | 1.0–4.0 | 0.061 |

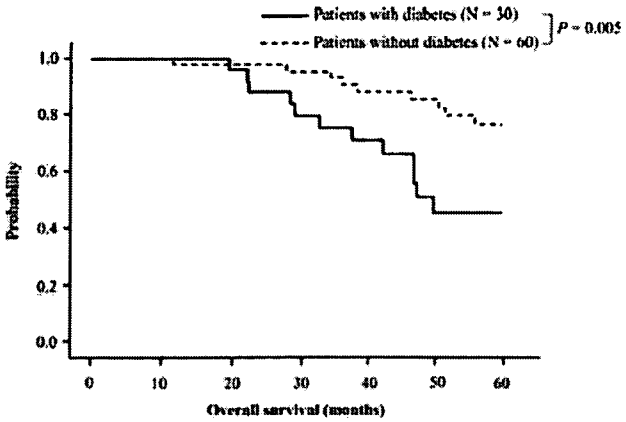


**Figure 2.** Kaplan-Meier curves for overall survival in the groups of patients with and without diabetes.

These curves indicated that overall survival rates were significantly lower in the diabetic patient group ($P = 0.005$).

### *Differential Impact of Diabetes on Prognosis After Surgical Treatment Between HBV- and HCV-Infected Patients*

Next, we classified the HCC patients into HBV- and HCV-related HCC patients, and examined the impact of diabetes on recurrence-free and overall survival rates after surgical treatment. We divided all patients into 25 HBs-Ag (+), HCV-Ab (−) patients (with HBV-related HCC) and 62 HBs-Ag (−), HCV-Ab (+) patients (with HCV-related HCC), and further divided these two groups of patients into four groups according to the presence or absence of diabetes. In 62 patients who were HCV-Ab positive, 53 patients were also positive for HCVRNA. The other 9 patients were not examined for HCVRNA. The clinical profiles of these four groups of patients are shown in Table 4. Three HBs-Ag (+), HCV-Ab (+) patients, who were not complicated by diabetes, were excluded from the analysis. There were no significant differences between the groups of HBV-related HCC patients with and without diabetes in age, gender, BMI, prevalence of alcohol abuse, platelet count, ALT, total bilirubin, Child-Pugh classification, liver fibrosis degree, tumor size, tumor differentiation degree, or the presence of vascular invasion, except for Alb and AFP. Similarly, there were no significant differences between the groups of HCV-related HCC patients with and without diabetes. The HbA1c levels were higher in the groups of diabetic patients with HBV- or HCV-related HCC.

The Kaplan-Meier curves for recurrence-free survival in the groups of HBV-related HCC patients with and without diabetes are shown in Figure 3. The recurrence-free survival rates 1, 3, and 5 yr after surgical treatment were 85.7%, 57.1%, and 42.9%, respectively, in the diabetic patient group, and 76.5%, 46.7%, and 40.0%, respectively, in the nondiabetic patient group, showing no significant differences between the two groups ($P = 0.596$, $P = 0.670$, and $P = 0.827$). In the analysis of overall survival in the groups of HBV-related HCC patients with and without diabetes by the method of Kaplan-Meier, it indicated that there was no difference between the two groups ($P = 0.505$) (Fig. 4).

Figure 5 shows the Kaplan-Meier curves for recurrence-free survival in the groups of HCV-related HCC patients with and without diabetes. The recurrence-free survival rates 1, 2, 3, 4, and 5 yr after surgical treatment were 75.0%, 38.9%, 22.2%, 11.1%, and 11.1%, respectively, in the diabetic patient group, and 94.6%, 83.9%, 62.1%, 35.0%, and 29.2%, respectively, in the nondiabetic patient group, indicating that the recurrence-free survival rates were significantly lower in the diabetic patient group than in the nondiabetic patient group ($P = 0.030$, $P < 0.001$, $P < 0.001$, $P < 0.001$, and $P < 0.001$).

In the analysis of overall survival in the groups of HCV-related HCC patients with and without diabetes, the overall survival rates 1, 2, 3, 4, and 5 yr after surgical treatment were 100%, 88.9%, 76.5%, 64.7%, and 43.8%, respectively, in the diabetic patient group, and 100%, 100%, 96.7%, 92.5%, and

**Table 4.** Characteristics of Patients With HBV- or HCV-Related HCC

| Characteristic | Patients With HBV-Related HCC | | | Patients With HCV-Related HCC | | |
|---|---|---|---|---|---|---|
| | With Diabetes (N = 8) | Without Diabetes (N = 17) | *P* Value | With Diabetes (N = 22) | Without Diabetes (N = 40) | *P* Value |
| Median age (yr) | 61.6 | 57.3 | 0.3 | 62.2 | 62.9 | 0.737 |
| Gender (male/female) | 7/1 | 13/4 | 0.5 | 17/5 | 35/5 | 0.302 |
| Body mass index (kg/m$^2$) | 23.4 | 23.2 | 0.9 | 23.5 | 22.7 | 0.348 |
| Alcohol abuse (+/−) | 2/6 | 6/11 | 0.6 | 11/11 | 21/19 | 0.853 |
| HbA1c (%) | 5.9 | 4.6 | 0.07 | 6.6 | 4.9 | <0.001 |
| Fibrosis (F1/F2/F3/F4) | 0/0/2/6 | 3/2/0/12 | 0.8 | 0/4/2/16 | 1/3/5/31 | 0.680 |
| Child-Pugh grade (A/B) | 6/2/0 | 15/2 | 0.4 | 18/4 | 35/5 | 0.551 |
| Platelet count (× 10$^4$/μL) | 11.5 | 13.9 | 0.3 | 12.4 | 13.5 | 0.520 |
| ALT (IU/L) | 31.8 | 42.3 | 0.6 | 84.2 | 63.5 | 0.233 |
| Total bilirubin (mg/dL) | 0.9 | 0.9 | 1.0 | 0.9 | 0.8 | 0.303 |
| Albumin (g/dL) | 3.8 | 4.2 | 0.02 | 4.2 | 4.2 | 0.983 |
| AFP (ng/mL) | 1,056 | 121 | 0.001 | 162 | 328 | 0.460 |
| Tumor size (mm) | 28.9 | 31.2 | 0.8 | 36.0 | 29.6 | 0.295 |
| Diff.degree (W/M/P) | 2/2/4 | 5/7/5 | 0.3 | 9/10/3 | 14/11/15 | 0.058 |
| Vascular invasion (+/−) | 1/7 | 4/13 | 0.5 | 12/10 | 15/25 | 0.548 |

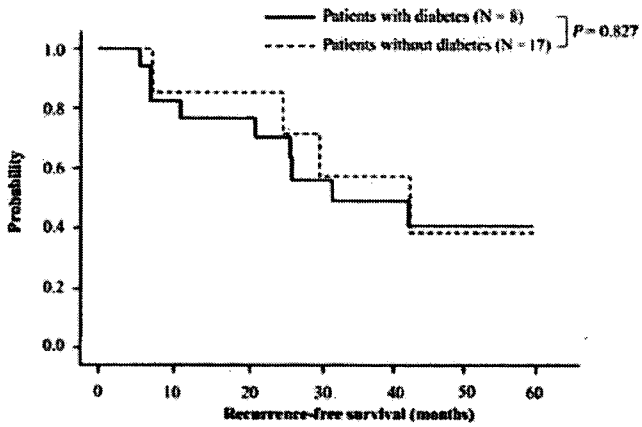


**Figure 3.** Kaplan-Meier curves for recurrence-free survival in HBV patients with diabetes and HBV patients without diabetes.

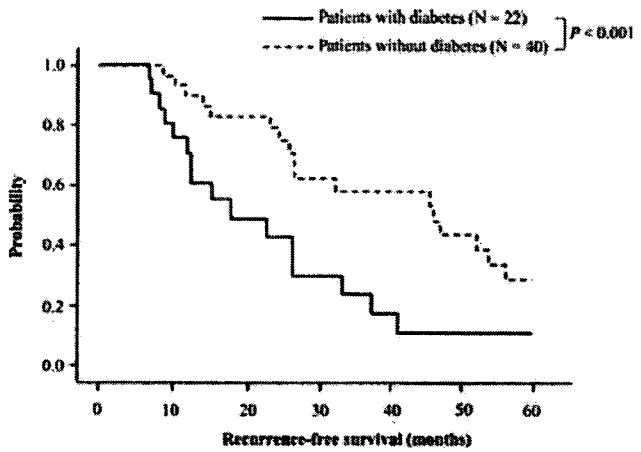


**Figure 5.** Kaplan-Meier curves for recurrence-free survival in HCV patients with diabetes and HCV patients without diabetes.

82.6%, respectively, in the nondiabetic patient group, indicating that the overall survival rates of more than 3 yr were significantly lower than in the nondiabetic patient group ($P = 1.000$, $P = 1.000$, $P = 0.035$, $P = 0.015$, $P = 0.004$) (Fig. 6).

***Factors Associated With Recurrence-Free Survival After Surgical Treatment for HCC in Patients With Diabetes***

Finally, we performed univariate and multivariate analyses to determine the variables that might affect the postoperative recurrence of HCC in the 30 HCC patients with diabetes, consisting of 17, 4, and 9 patients receiving insulin therapy, oral hypoglycemic drugs, and no treatment, respectively. Univariate analysis identified Child-Pugh classification B as a factor significantly contributing to the postoperative recurrence of HCC ($P < 0.001$) (Table 5). When we conducted multivariate analysis, we chose variables that had been already pointed out as a risk factor for HCC recurrence and whose $P$ value was lower than 0.1 in univariate analysis. Multivariate analysis identified Child-Pugh classification B (risk 40.0, 95% CI 4.4–362.1, $P = 0.001$) and the presence of insulin therapy (risk 3.9, 95% CI 1.0–15.3, $P = 0.049$) as factors significantly contributing to the postoperative recurrence of HCC (Table 6). In multivariate analysis, both factors showed significant $P$ value. Based on the results, we considered that both factors contribute to recurrence of HCC independently.

## DISCUSSION

In the present study, univariate and multivariate analyses identified the presence of diabetes as a factor significantly contributing to the recurrence of HCC after surgical treatment. The results are consistent with the findings of Ikeda *et al.* (12). They analyzed a population of 64 HBV-related HCC patients and a larger population of 144 HCV-related HCC patients, but did not compare the postoperative recurrence rate between the two populations. In our study, 25 and 62 patients with HBV- and HCV-related HCC, respectively, were included, similar to the proportion of such patients in the study by Ikeda *et al.* (12), presumably leading to similar results. On the other hand, none of the variables that have been reported to contribute to the postoperative recurrence of HCC, such as liver fibrosis degree, Alb level, AFP level, tumor differentiation degree,

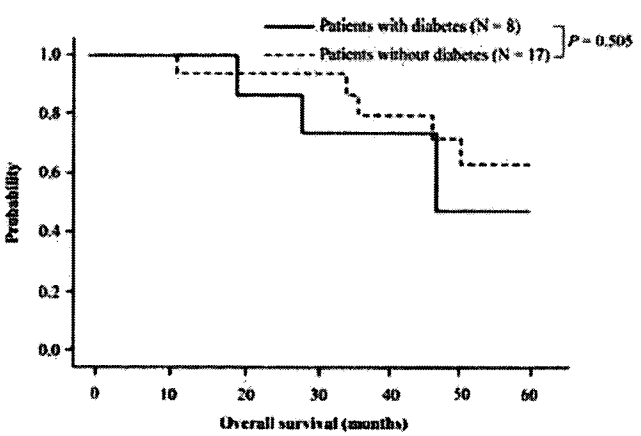


**Figure 4.** Kaplan-Meier curves for overall survival in HBV patients with diabetes and HBV patients without diabetes.

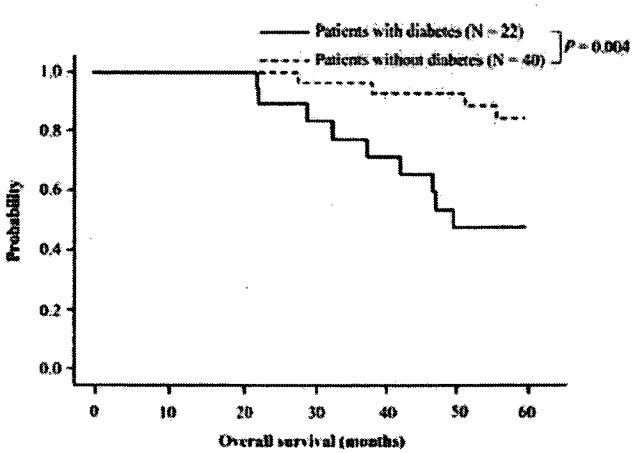


**Figure 6.** Kaplan-Meier curves for overall survival in HCV patients with diabetes and HCV patients without diabetes.